TECTONIC IMPLICATIONS OF THE MAY 18, 1971 ARTYK EARTHQUAKE, NORTHEAST RUSSIA

By

Melissa S. McLean

A THESIS

Submitted to
Michigan State University
In partial fulfillment of the requirements
For the degree of

MASTER OF SCIENCE

Geological Sciences

2009

ABSTRACT

TECTONIC IMPLICATIONS OF THE MAY 18, 1971 ARTYK EARTHQUAKE, NORTHEAST RUSSIA

By

Melissa S. McLean

The Artyk earthquake of May 18, 1971, is the largest earthquake in continental northeast Russia in the instrumental era. An extensive aftershock sequence occurred during the three months following the mainshock. 286 of these events were relocated using an expanded data set incorporating data from both temporary and regional stations, and using a local travel-time curve.

The relocated aftershocks align very closely with the Kobdi fault as mapped by Shilo (1961) and form two clusters. The northern cluster has the same strike as the northwest-striking nodal plane of the focal mechanism, indicating left-lateral strike-slip movement. The southern cluster shows a bend to the east. The Kobdi fault appears to offset a diorite by about 8 km, yielding an inferred rate of motion of 0.2 cm/yr on the fault.

The left-lateral strike-slip nature of the mainshock, the northwest-striking aftershock distribution, and the lack of faults with a southwest or east to northeast strike, and recent activity on the Ulakhan fault to the northeast imply the earthquake cannot lie on the North America – Okhotsk or Okhotsk – Eurasia plate boundaries or at a triple junction between them. Instead, the Artyk earthquake was generated along a fault that represents internal deformation in the Okhotsk plate.

I dedicate this work to my son, Anthony.

ACKNOWLEDGEMENTS

Kaz Fujita, this wouldn't have been possible without you. I sincerely appreciate all of the hard work you put into teaching and guiding me through graduate school, and the many steps you took to bring me back so that I could properly finish. I can't thank you enough.

Kevin Mackey, your optimism and unique way of looking at things were instrumental in my understanding of northeast Russia. I truly enjoyed our trip to Russia and I look forward to stories of your future adventures around the world.

Bill Cambray and Dave Hyndman, thanks for being a part of my committee. You have both helped me understand things in a different way, for which I am thankful!

Jackie Bennett, your knowledge of the system really helped me get through the bureaucracy so I could finish. I appreciate it.

Martha and Elizabeth Fujita, you guys were my family away from home. I appreciate the tremendous hospitality and the love you showed me, as if I was a member of your family.

Rob McCaleb, you were a great roommate and are a wonderful friend. I like to think that our band practices were instrumental in understanding our school work.

To my colleagues in Russia: Boris Koz'min for your experience and knowledge. Larissa Gunbina and folks at the Magadan seismic station for your hospitality.

To my friends, there are too many of you to thank here, but know that you all made a big difference in getting me through some long years.

Mom and Dad, thanks for the financial backing and the support so that I could go to graduate school in the first place. Shannon and Jenny, thanks for reminding me that school is important, but family is even more important.

And last, I want to thank my husband, Larry, and my son, Anthony, for putting up with me finishing school. I love you both.

This research was supported, in part, by the Department of Geological Sciences of Michigan State University, National Science Foundation grant OPP 98-06130, and the Department of Energy contract DE-FC03-02SF 22490, and is gratefully acknowledged.

TABLE OF CONTENTS

LIST OF TABLES

LIST OF FIGURES

Images in this thesis are presented in color.

Chapter 1: Introduction

The present-day plate boundary between North America and Eurasia is well studied and understood in the North Atlantic and Arctic Ocean basins where it is located along the Mid-Atlantic and Gakkel ridges. Details of how it continues into the northeast Asian continent and its specific location between the Arctic and Pacific oceans, however, have remained less well understood. This segment of the plate boundary is one of the last frontiers in understanding the framework of global plate movements.

The location of the plate boundary in northeast Russia lies within a zone of seismicity known as the Chersky Seismic Belt (CSB; e.g., Koz'min, 1984, Parfenov et al., 1988; Fujita et al., in press). This is a wide zone that, loosely defined, extends some 2000 km from the Laptev Sea of the Arctic Ocean to northern Kamchatka and Sakhalin Island (Figure 1-1). It is an intracontinental convergence zone and, like similar regions elsewhere, exhibits considerable complexities with the possibility of numerous blocks or microplates, and wide zones of diffuse deformation (Jackson and McKenzie, 1988; England and Jackson, 1989; Gordon, 1998).

Previous plate boundary studies within northeast Russia have focused on the location and relative motions occurring between the North American and Eurasian plates and the existence of an Okhotsk microplate (e.g. Chapman and Solomon, 1976; Savostin and Karasik, 1981; Savostin et al., 1982; Cook et al., 1986; Fujita et al., 1990a; Parfenov et al., 1988; Riegel et

Figure 1-1. Seismicity map of eastern Russia based on MSU Eastern Russia Seismicity Database. Events in the Aleutian Islands are not included in the database and are not shown. Dots are proportional to event size (inset). Older events (pre-1960) are shown as grey dots without outline. The locations of the Chersky Seismic Belt (CSB) and Olekma-Stanovoi Belt (OSB) are shown in yellow shading. The epicenter of the Artyk earthquake of May 18, 1971 is labeled.

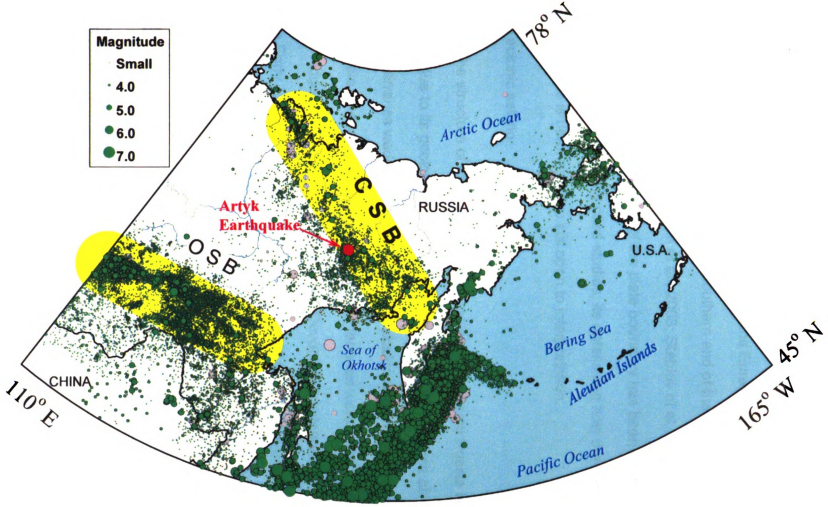
Magnitude
Small
4.0
5.0
6.0
7.0
78° N
Arctic Ocean
RUSSIA
Artyk
Earthquake
C S B
O S B
U.S.A.
Bering Sea
Sea of
Okhotsk
Aleutian Islands
45° N
CHINA
110° E
165° W
Pacific Ocean

al., 1993). The region is understood to represent a zone of diffuse compression (e.g., Imaev et al., 1990; Fujita et al., 1990a, in press) resulting from the convergence of the North American and Eurasian plates rotating around an Euler pole located near the southern end of the Laptev Sea (Figure 1-2; e.g., Cook et al., 1986; Calais et al., 2003; Steblov et al., 2003). Although the general location and nature of the plate boundary has been relatively well determined in the previously cited studies, its details and how the northern Okhotsk plate is deforming are still open to interpretation.

1.1 Tectonic setting

The structure of the plate boundary region in northeast Russia is very complex due to its geological history. Spatially, it lies within a zone of accreted terranes wedged between the stable platforms of the North America and Eurasia. Recent studies suggest that the terranes were rifted from the eastern edge of the Siberian platform in the Devonian, amalgamated offshore in the Early Jurassic and reaccreted to the edge of the platform in the Late Jurassic (Nokleberg et al., 2000; Parfenov and Kuz'min, 2001). In the Cenozoic the present-day plate boundary developed through northeastern Russia that, with the opening of the Eurasia basin of the Arctic Ocean, resulted in general compression and the southward extrusion of the Okhotsk microplate (Cook et al., 1986).

Figure 1-2. Generalized tectonic map of northeastern Russia. Solid green lines show boundaries of major plates and blocks. Dashed lines show minor boundaries and the light green shaded area represents the region of high deformation in the northern Okhotsk plate. Arrows show directions of relative plate motion. The Artyk earthquake is labeled. Plates: NA = North American; EU = Eurasian; OK = Okhotsk, PA = Pacific. Blocks: LA = Laptev; AM = Amur; BE = Bering. Representative focal mechanisms are shown as lower hemisphere projections with the compressional quadrants shaded. Approximate location of North America - Eurasia pole is shown by shaded yellow dot. After Fujita et al. (in press).

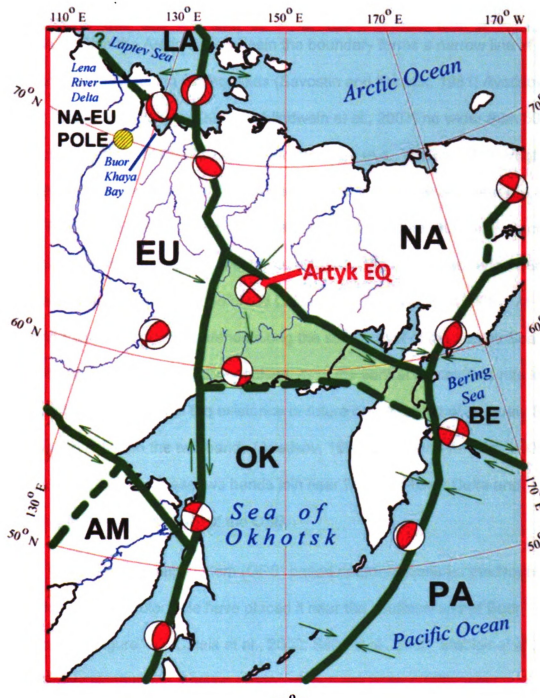
110° E
130° E
150° E
170° E
170° W
70° N
60° N
50° N
130° E
150° E
Laptev Sea
LA
Lena
River
Delta
NA-EU
POLE
Buor
Khaya
Bay
Arctic Ocean
EU
NA
Artyk EQ
Bering
Sea
BE
OK
Sea of
Okhotsk
AM
PA
Pacific Ocean

The present-day North America-Eurasia plate boundary extends along the Mid-Atlantic Ridge through Iceland and then northward to the Arctic Ocean. Within the Arctic Ocean basin the boundary forms a narrow line of primarily normal-faulting earthquakes (Savostin and Karasik, 1981; Avetisov, 1996; Engen and Eldholm, 2003; Schlindwein et al., 2007) no wider than 50 km, following the Gakkel (Arctic) Mid-Ocean ridge (e.g., Wilson, 1963; Vogt et al., 1979; Cochran et al., 2003), which extends to the Laptev Sea near the Lena River delta. In the continental shelf of the Laptev Sea, the zone of active seismicity is offset to the east and forms a band along the eastern edge Buor Khaya Bay at the southern end of the Laptev Sea (Fujita et al., 1990b). A second band of seismicity extends along the south coast of the Laptev Sea. This, combined with the relative aseismicity of the central Laptev Sea has led some workers to propose the existence or future development of a Laptev Sea microplate between the two bands (Avetisov, 1993, 2000; Franke et al.,2000; Imaev et al., 2003). These two bands join near the Lena River Delta and merge with the earthquakes of the CSB.

Global positioning system (GPS) based determinations for the North America-Eurasia Euler pole have placed it near the southern end of Buor Khaya Bay (Figure 1-2; Calais et al., 2003; Sella et al., 2002; Steblov et al., 2003), very close to the location proposed by Cook et al. (1986) using earthquake slip vectors. The present-day Euler pole location implies that there is extension to the north in the Laptev Sea, and convergence to the south in the CSB and the Sea of Okhotsk region, as first recognized by Wilson (1963).

South of Buor Khaya Bay, the earthquakes change to predominantly thrust events with convergence between North America and Eurasia. How this convergence south of the Euler pole is accommodated is not entirely understood. Most studies recognize a separate Okhotsk plate (Figure 1-2) being extruded to the southeast (Savostin and Karasik, 1981; Savostin et al., 1983; Cook et al., 1986; Riegel et al., 1993; Fujita et al., 1990, 1997, in press; Imaev et al., 1990, 2000; Parfenov et al., 1988). Large strike-slip faults striking along and parallel to the proposed North America-Okhotsk plate boundary (Figure 1-3), which Gusev (1979) has named the "Indigirka-Kolyma" system of faults have been mapped through geological surveys and satellite image interpretation. Features such as slickenlines, mylonites, zones of crushed rocks and river offsets evidence of the strike-slip nature of many of these faults. Linear magnetic anomalies and sharp gradients in the gravitational field further verify the location of these faults (e.g. Vashchilov, 1963; Gusev, 1979; Imaev et al., 1990, 2000).

The seismicity becomes very diffuse south of the Euler pole, indicating that the region is actively deforming. This deformation has been suggested to be the result of distributed deformation and thrusting (e.g. Bobrovnikov and Izmailov, 1989), rigid extrusion (e.g. Riegel et al., 1993) or a combination of the two (Hindle et al., 2006, in press).

In the central CSB, earthquakes appear to branch off into two zones (Figure 1-1), which strike NW-SE, parallel to the southern Chersky Mountains

Figure 1-3. Map of major faults and lineaments in the central CSB. Dashed lines represent faults whose location or existence is less certain. Thrust faults are shown by toothed lines (teeth on upper plate). Blue dot shows location of Artyk earthquake.

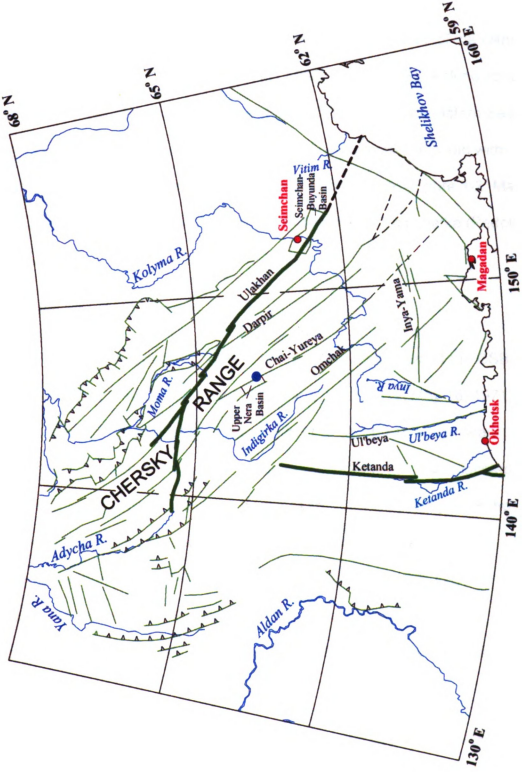
68° N
65° N
62° N
59° N
160° E
150° E
140° E
130° E
Sheikhov Bay
Yitim R.
Seimchan
Seimchan-Buyunda Basin
Kolyma R.
Ulakhan
Darpir
Magadan
Inya-Yana
Chai-Yureya
Omchak
CHERSKY
RANGE
Moma R.
Upper Nera Basin
Indigirka R.
Inya R.
Okhotsk
Ul'beya
Ul'beya R.
Ketanda
Ketanda R.
Adycha R.
Yana R.
Aldan R.

and the Ulakhan fault, and N-S, parallel to the Sette Daban Range and the Ketanda fault system (Figure 1-3; Imaev et al, 1990, 2000; Fujita et al., in press). These zones are believed to represent the boundaries of the Okhotsk plate (Parfenov et al., 1988; Riegel et al., 1993). The NW-SE striking zone of seismicity follows the Chersky Range (Figure 1-3) to the northeastern Sea of Okhotsk and continues further across the neck of Kamchatka to join with earthquakes delineating the edge of the Bering microplate (Figure 1-2; Mackey et al., 1997) and possible convergence off of northeast Kamchatka (Pedoja et al, 2006).

1.2 Statement of the Problem

The largest earthquake (Mw 6.4) in the continental part of the CSB in the modern instrumental era (1962 to present) occurred on May 18, 1971, in its central part (Parfenov et al., 1988; Fujita et al., in press), a significant distance off of either of the two branches described above. It was located within a broader zone of seismicity encompassing the northern part of the Okhotsk plate which has been suggested to be a region of elevated deformation (Figure 1-2; Fujita et al., in press). Because of its size and location, its tectonic nature is important to understanding the plate configuration and interactions between the North American and Eurasian plates.

As noted above, numerous faults have been mapped in the CSB (Figure 1-3; e.g., Larina, 1960; Shilo, 1961; Kurushin, 1976; Surmilova et al.,

1986; Imaev et al., 2000; Smirnov, 2000). Unfortunately, it is uncertain which faults are active because previously located epicenters were less accurate, due to methodologies used by Russian networks, a lack of data sharing between networks, and a lack of western access to their local data. When faults were mapped, no distinction was made between whether a fault was active or ancient. This, coupled with the low-resolution of available mapped geology, makes it impossible to develop meaningful conclusions regarding exactly where and how the Okhotsk plate is deforming.

The Artyk earthquake of May 18, 1971, presents a unique opportunity to further study this problem. The earthquake was accompanied by an extensive aftershock sequence that lasted several months. A four station temporary network was deployed in the area by the Yakutian Institute of Geological Sciences (YIGS, now the Institute of Diamond and Precious Mineral Geology) and the Yakutsk Experimental Methodological Seismological Division (Yakutsk EMSD; now the Yakut Affiliate of the Siberian Division of the Geophysical Survey of Russia; hereafter Yakut regional network) and the Northeast Interdisciplinary Scientific Research Institute (NEISRI) and the Magadan Experimental Methodological Seismological Division (Magadan EMSD; now the Magadan Affiliate of the Geophysical Survey of Russia; hereafter Magadan regional network) . The aftershock sequence provides a data set which allows an opportunity to accurately map active faulting within a part of this complicated region.

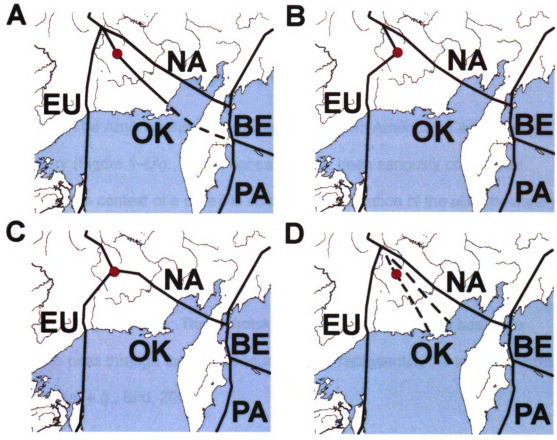

Figure 1-4. Schematic diagrams showing possible plate configurations relative to the Artyk earthquake (red star). a. Artyk event is located on NA-EU plate boundary, which may be changing location. b. Artyk event is on EU-OK plate boundary. c. Artyk event is located at triple junction between NA, EU, and OK. d. Artyk event represents an intraplate event in OK which is breaking into blocks under compression between NA and EU.

The Artyk earthquake has been proposed to represent one of four possibilities in the context of an extruding Okhotsk plate being compressed and deformed between its larger neighbors:

1. The Artyk earthquake occurs on the North America – Okhotsk plate boundary (Figure 1-4A). This proposal has not been seriously considered except in the context of a possible change in the location of the plate boundary (Fujita et al., 2002).

2. The Artyk earthquake occurs on the Okhotsk – Eurasia plate boundary (Figure 1-4B). The Okhotsk – Eurasia plate boundary has been drawn to pass through the Artyk sequence as it represented the largest events in the area (e.g., Bird, 2003).

3. The Artyk earthquake cluster represents a triple junction between the Okhotsk, North American and Eurasian plates (Figure 1-4C; Imaev et al., 2003).

4. The Artyk earthquake occurs along a fault internal to the Okhotsk plate that is accommodating intraplate deformation (Figure 1-4D; Hindle et al., in press).

In this thesis I relocate aftershocks of the Artyk earthquake and use satellite, topographic, and geologic data to determine which mapped local fault(s) were ruptured by this earthquake and the implications this would have

for the resolution of the above scenarios within the context of deformation in the North America – Eurasia plate boundary zone.

Chapter 2: The Artyk Earthquake and its Regional Tectonic Setting

2.1 The Artyk Earthquake of May 18, 1971

2.1.1 Hypocenter and Origin Time

The Artyk earthquake occurred at approximately 7:45 AM local time (22:44:49 UTC) near the settlement of Artyk (Figure 2-1) in the Oimyakon Uluus of the Sakha Republic (Yakutia) of the Russian Federation (formerly the Yakut Autonomous Soviet Socialist Republic of the Soviet Union). The earthquake was initially called the Oimyakon earthquake by Yakutian seismologists. The epicentral region is located on the northeastern side of the Upper Nera basin, along the Chai-Yureya Fault (Imaev et al., 2003; see further below).

The epicenter was initially located by using arrivals at ten stations of the Yakut regional network operated by the Yakutian Institute of Geological Sciences (YIGS) and the Magadan regional network operated by the Northeast Interdisciplinary Scientific Research Institute (NEISRI; see section 3.1). These data were later supplemented by that of the Soviet national network and subsequently from international global networks (Figure 2-2; Table I).

We relocated the epicenter using a local crustal model developed by Mackey (1999) (see section 4.1). The resulting relocated epicenter (Solution 12, Table I; see section 4.4.1) calculated using regional and teleseismic data

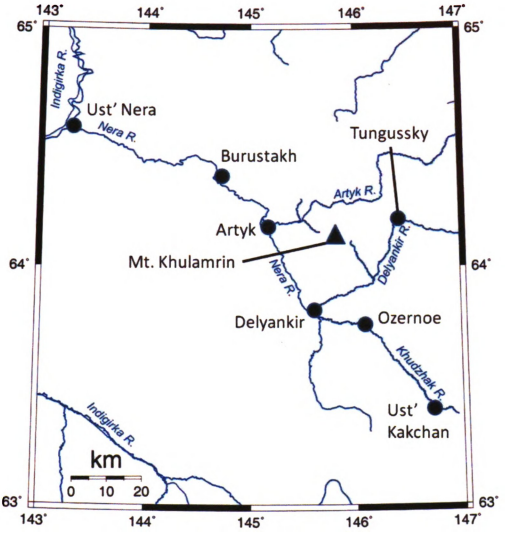

Figure 2-1. Index map of the local study area. Settlements are represented by black dots. Mt. Khulamrin represented by black triangle.

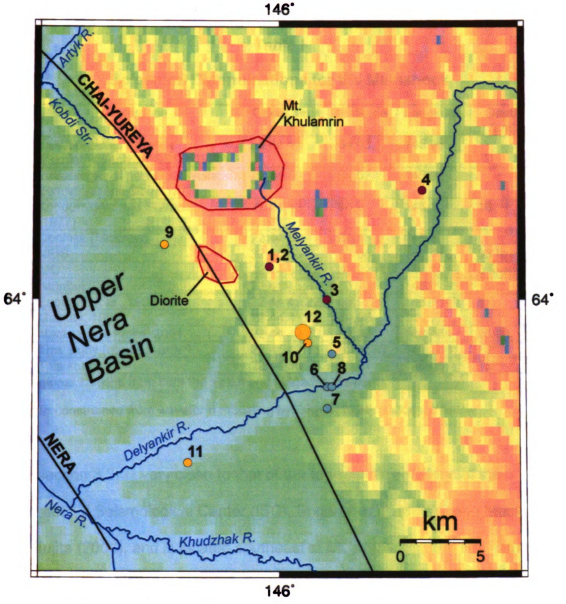

Figure 2-2. Comparison of epicentral determinations for the Artyk mainshock (numbers refer to solutions listed in Table 1). Russian solutions shown as red dots. Teleseismic solutions as blue dots. MSU solutions as orange dots. Best solution is shown by larger orange dot. The diorite of Mt. Khulamrin and an outlier exposure are shown by the red outlines.

Table I

Epicentral Determinations for the Mainshock

ID	Reference	Origin Time (UTC)	Latitude	Longitude	Depth (km)
1	Yakut regional network (Zemletryaseniya v SSSR 1971)	22 44 43	64.03	145.98	
2	Yakut regional network (Byulletin' Zemletryasenii Sibiri, 1973)	22 44 49.5	64.03	145.98	
3	Kondorskaya and Shebalin (1977)	22 44 43	64.0	146.1	16
4	Obninsk (Moscow)	22 44 38	64.1	146.3	
5	NEIS	22 44 43.8	63.95	146.112	33 fixed
6	ISC	22 44 39.25	63.9211	146.1013	0 fixed
7	Istanbul (ISK)	22 44 43.8	63.9	146.1	
8	Engdahl et al., 1998	22 44 42.22	63.9229	146.1149	8.5
9	Mackey, 1999	22 44 41.90	64.05	145.76	33.1
10	Mackey and Fujita, 2001	22 44 42.23	63.960	146.064	20.85
11	This study (regional only*)	22 44 42.11	63.8530	145.8081	13**
12	This study	22 44 39.23	63.97	146.05	13**

* all regional stations from both the Yakut and Magadan networks.

** Depth constrained from waveform modeling by Riegel (1994) discussed below.

(see section 3.2) is very close to that of the teleseismic solutions of the International Seismological Center (ISC), Engdahl et al. (1998), and Mackey and Fujita (2001), and is located southeast of Mt. Khulamrin and lies near the mapped trace of the Chai-Yureya Fault. It falls latitudinally between the regional and teleseismic determinations and slightly to the west of other solutions. The relationship of the mainshock to the aftershock sequence is discussed in section 4.4.1.

All epicentral determinations (Table I) place the Artyk earthquake within several kilometers of the trace of the Chai-Yureya as mapped by Imaev et al. (2003; see also sections 2.2.3 and 5.1).

Focal depths (Table I) calculated using teleseismic stations are generally unreliable; the ISC depth is fixed at 0 and the NEIC depth is fixed at 33 km. Engdahl et al. (1998), Mackey (1999), and Mackey and Fujita (2001) calculated depths using teleseismic and regional P-wave arrivals; Mackey (1999) and Mackey and Fujita (2001) also used Sg phases. Results from these studies converged to crustal depths, but still differ greatly from each other (8 – 30 km). Riegel et al. (1993) constrained the focal depth using long-period waveform modeling at 13 km (see section 2.1.3); earlier modeling by McMullen (1985) obtained a depth of 10 km. We adopted the Riegel et al. (1993) solution of 13 km in relocating the mainshock. It is mid-way between the high quality Engdahl et al. (1998) relocated depth (8 km) and the Kondorskaya and Shebalin (1977) solution at 16 km. The Yakut regional network did not calculate a focal depth for this event.

2.1.2 Magnitude and Energy

Estimates of the magnitude of the Artyk earthquake have varied between 5.8 and 7.1 (Table II), depending on the author and method used.

In order to better quantify the magnitude of the event, Fujita et al. (2002) used World-Wide Standardized Seismograph Network (WWSSN) long

Table II

Magnitude of the Mainshock

Reference	Type	Value
Yakutsk regional network	M_L	7.1
Zemletryasenia v SSSR (Kondorskaya and Shebalin, 1977)	m_{PV}	6.8
Zemletraseniya v SSSR	m_{PV} – SKM-3 (short period)	6.5
Obninsk	M_b	6.4
NEIC	M_b	5.8
ISC	M_b	5.9
Obninsk	m_S	6.9
NEIC	m_S	6.6
Fujita et al. (2002); adopted in this study	M_w	6.4

period analog the seismograms (Figure 2-3) from eight stations to calculate a moment for this event using the method of Okal and Talandier (1989). Vertical component seismograms from WWSSN stations COR, PMG, STU, GUA, TRN, ESK, LEM, and STJ were digitized and moments were calculated for various periods of 50 to 200 seconds at each station. The results were corrected for the focal mechanism using the solution of Riegel et al. (1993; see section 2.1.3) and averaged over the various periods. The results at the individual stations were very robust except for LEM, which is located near a nodal plane, thus small errors in the azimuth of the nodal plane would have large effects on the focal mechanism correction; thus the station was omitted. The final results for the seven remaining stations were averaged to obtain a seismic moment, M_0, of $5.1 \pm 0.1 \times 10^{25}$ dyne-cm, and a corresponding M_w of

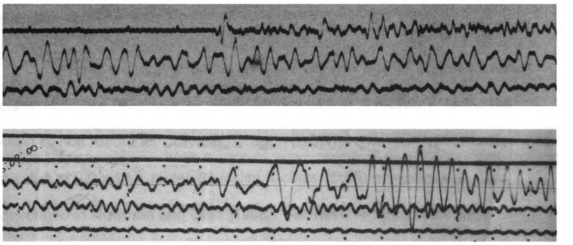

Figure 2-3. Sections of representative vertical component WWSSN long-period analog seismograms showing surface waves digitized by Fujita et al. (2002) to calculate the seismic moment of the Artyk earthquake. (top) Corvallis, Oregon; (bottom) St. Johns, Newfoundland. Tick marks every minute.

6.4. An earlier estimate by Filson and Frasier (1972) was approximately 10^{25} dyne-cm.

The initial energy estimate by the YIGS was 3 x10^{16} Joules (Russian K-class 16.5; see Rautian et al., 2007 for discussion of K-class). Using the short-period record for Corvallis, Oregon (COR), Fujita et al. (2002) calculated a value of 9.0 x 10^{15} Joules (Russian K-class 15.95) using the algorithm described in Newman and Okal (1998). As these two estimates were essentially identical, they did not calculate additional stations.

These analyses make the Artyk event the largest well-documented event in the Chersky Seismic Belt in the modern instrumental period, although significantly smaller than the magnitude of 7.1 often cited by Russian authors (e.g., Imaev et al., 2000).

2.1.3 Focal Mechanism

The focal mechanism for this earthquake has been determined by a number of authors using a variety of techniques. The solutions are all nearly identical (Table III) and indicate that the solution is very robust.

Due to its comprehensive nature of the data used, the solution by Riegel et al. (1993; Figure 2-4) is adopted as most reliable for this event. They used long-period P-wave first motions re-read from WWSSN records

Table III

Focal Mechanism Determinations for the Mainshock

Reference	Method	Strike-1	Dip-1	Rake-1	Strike-2	Dip-2	Rake-2
McMullen, 1985	Synthetic seismograms and WWSSN P-wave first motions	303	82	2	213	88	172
Chapman and Solomon, 1976	P wave first motions	313	83	7	223	89	173
Filson and Fraser, 1972	P-wave and surface wave inversion	325	90	0	235	90	180
Koz'min, 1984	Regional and bulletin P-wave first motions	308	86	9	218	81	176
Koz'min et al., 1975	Regional P-wave first motions	327	90	0	237	90	180
Franke et al., 2000	P-waves	329	76	14	236	77	165
Riegel et al., 1993; Riegel, 1994	Long-period synthetic seismograms and P-wave first motions	305	82	6	214	84	172
Balakina et al., 1993	Regional and bulletin P-wave first motions	314	72	12	220	79	162

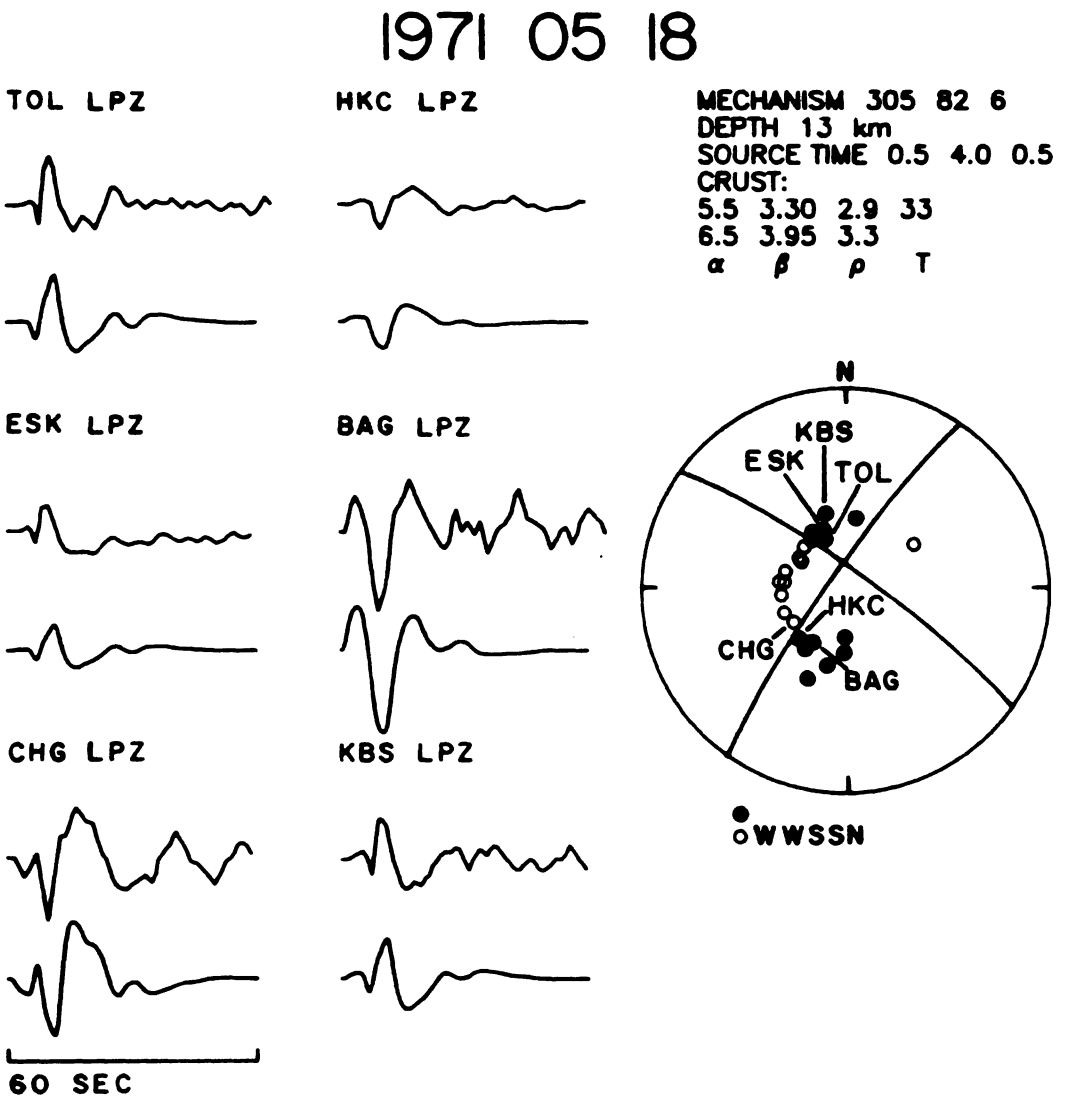

Figure 2-4. Focal mechanism of the Artyk mainshock using synthetic seismograms modeling of long-period WWSSN records (Riegel et al., 1993). Upper trace for each station is the observed record, the bottom trace is the synthetic. The parameters of the crustal model are given at upper-right (α is P-wave velocity in km/sec, β is S-wave velocity in km/sec, ρ is density in gm/cm^3, and T is layer thickness in km). Stereogram shows lower-hemisphere projection of first motions re-read from WWSSN seismograms; open circles are dilitations, solid circles are compressions.

(including those from McMullen, 1985), regional P-wave first motions from Koz'min (1984), and synthetic seismogram modeling using the method of Kroeger (1987). They calculated regional take-off-angles using the Jeffreys and Bullen (1940) velocity model which Mackey (1999) showed was a very good first approximation for the region.

The calculated strikes (305°-327°) of the northwest striking nodal plane cluster about the strike of the Chai-Yureya Fault (314°) in the epicentral area (see section 2.2.2) and therefore is presumed to be the fault plane. Thus the focal mechanism is almost pure strike-slip and represents left-lateral faulting on a northwest-southeast striking plane. The dip angle is very steep (72-90°), with an average around 83°, close to the 70-75° dip on the fault cited by Smirnov (2000).

Filson and Frasier (1972), using long-period WWSSN waveforms, determined that the rupture propagated to the northwest over a distance of 40 km at 4-5 km/sec.

2.1.4 Macroseismic Data

Immediately after the Artyk earthquake, scientists from the Institute of the Earth's Crust (IEC, Irkutsk), YIGS, and NEISRI jointly collected macroseismic data using interviews and mail questionnaires (Koz'min et al., 1975; Kurushin et al., 1976; Koz'min, 1984). These felt reports are summarized below.

The total felt area of the earthquake was over 900,000 km^2 (Figure 2-5). The maximum intensity (MSK 1964 scale; similar to Modified Mercalli) of the earthquake (VIII) was reported by a temporary geological field survey station, 30 km north-northwest of the epicenter. Here the earthquake was felt by all. People ran out of buildings and the sound from the earthquake drowned out that of a running tractor. In a wooden house, a table was overturned, objects fell from shelves, and all the windows were broken. Intensity VII was reported from the settlements of Artyk, Delyankir, Burustakh, Ozernoe, and parts of the inactive Tungussky mine (Figure 2-1). Near the settlement of Ozernoe, heavy drilling equipment was moved one meter. In Delyankir, two brick lined kilns were destroyed. Heavy furniture moved in homes, plaster collapsed, and people struggled to stay standing. Similar effects occurred at Burustakh. In Artyk, northwest of the epicenter, the earthquake began with strong vibrations accompanied by a muffled rumble and a column of dust rose into the sky. The top of the chimney of the central boiler plant swayed with an amplitude of three meters. In the repair shop of the Artyk truck base, a three meter high ventilation chimney collapsed and in the main building, thin, cracks formed in the walls and plaster broke off. Standing automobiles rocked as if driven forwards and backwards. Dishes were broken and books fell off shelves at all four settlements. At Tungussky, mine logs forming the ceiling of the workings fell. On the Ust' Nera to Magadan highway (Figure 2-5), numerous rockfalls from steep hillsides were observed between Artyk and Ust'Nera.

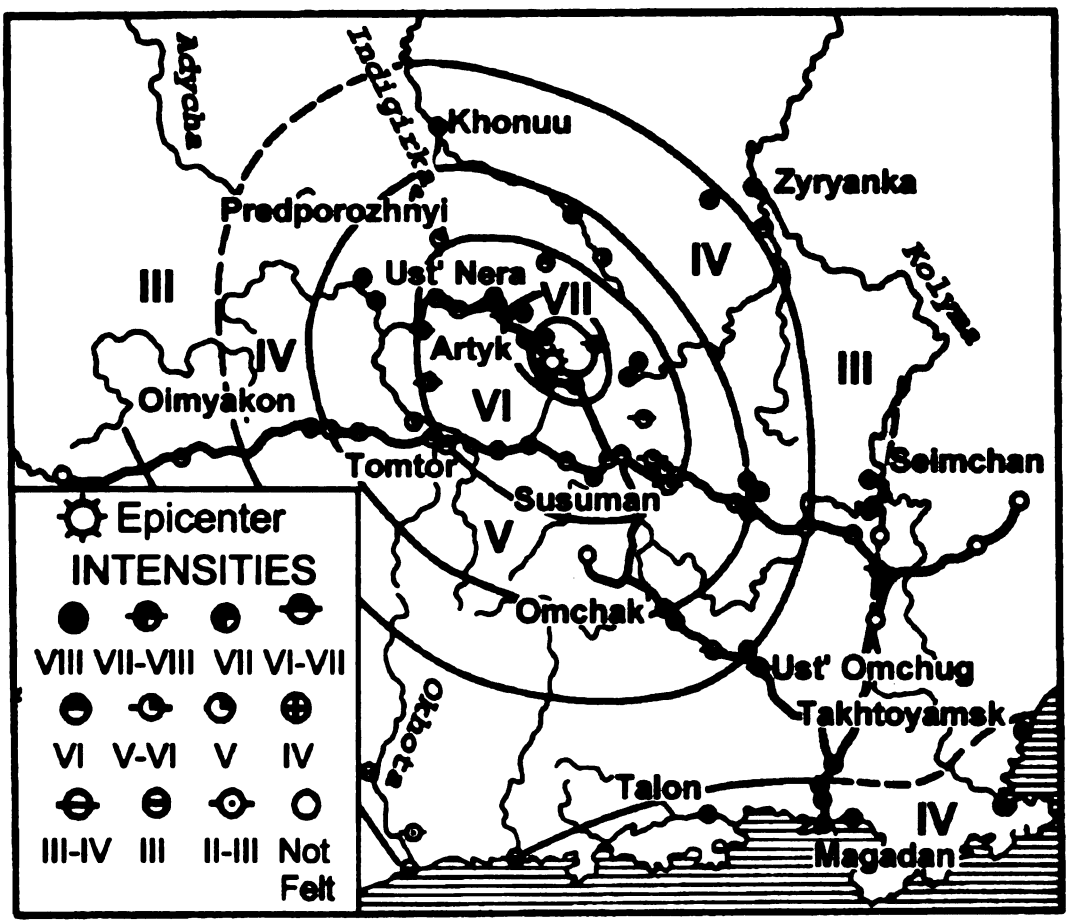

Figure 2-5. Intensity map of the main shock (Kurushin et al., 1976): 1 – main shock epicenter; 2 – area of ground deformation; Intensity of shaking, in points (MSK scale): 3 – greater than VIII; 4 – VII to VIII; 5 – VII; 6 – VI to VII; 7 – VI; 8 – V to VI; 9 – V; 10 – IV; 11 – III to IV; 12 – III; 13 – II to III; 14 – not felt.

Intensity VI was noted at Ust' Nera, Tomtor, Susuman and elsewhere at a distance range of 150-170 km. The earthquake was felt by all inhabitants indoors and by many outdoors. People ran out of their homes and thin cracks formed in plaster. Crockery and window panes rattled, objects on tables and shelves fell, and furniture moved. A rumble from underground was heard at distances up to 170 km (Koz'min et al., 1975).

The earthquake was felt with intensity V at Oimyakon, Predporozhnyi and other localities at distances of 200-250 km. Windows, plates, and crockery rattled and shelves and ceilings squeaked. Chandeliers vibrated and books fell from shelves. In Predporozhnyi, paint was shaken off of walls and plaster cracked.

In the intensity IV zone (Zyryanka, Khonuu and elsewhere) the earthquake was felt on the first floor of structures but rarely by those outside. Crockery, windows, and bookcases rattled. Hanging chandeliers oscillated and some objects moved.

Intensities elevated by one unit were noted along the coast of the Sea of Okhotsk (e.g., Magadan, Talon and Takhtoyamsk). Kurushin et al. (1976) interpret this increase as a result of the presence of discontinuous, as opposed to the regional continuous, permafrost. Alternatively, this may simply be a result of increased unconsolidated sediment thickness near the coast or of higher population density and the presence of larger buildings.

The isoseismals of the Artyk earthquake (Figure 2-5) are generally ellipsoidal in form, with the major axis approximately aligned with the orientation of both the fault plane and the strike of Mesozoic and Cenozoic structures of the Verkhoyansk-Kolyma fold system (Kurushin et al., 1976; Koz'min et al., 1975).

The Yakut network-calculated mainshock was located about 15 km southeast of the region with highest intensities as determined by landslides and surface ruptures (Kobdi Stream; Figure 2-2; see section 2.1.5).

2.1.5 Landslides and Surface Ruptures

Aerial surveys and field observations were conducted by the IEC near the mainshock epicenter to search for landslides and surface ruptures (Kurushin et al., 1976; Koz'min, 1984). No faulting associated surface ruptures were observed but massive disruptions of the surface vegetation layer were observed with mass movements into the Kobdi Stream valley over an area of about 18 km^2 (Figure 2-6 and Figure 2-7). Large amounts of material consisting of soil, water, and snow, formed cone-shaped mud flows with a thickness of up to 5-6 m, especially at the mouths of the tributaries of the Kobdi Stream (Figure 2-7). The landslides and debris cones are variable in shape and they ranged from a few square meters up to 20,000 m^2 in size. The total area of the landslides in the Kobdi Stream valley was about 250,000 m^2 with a volume of displaced material reaching over 100,000 m^3. Because

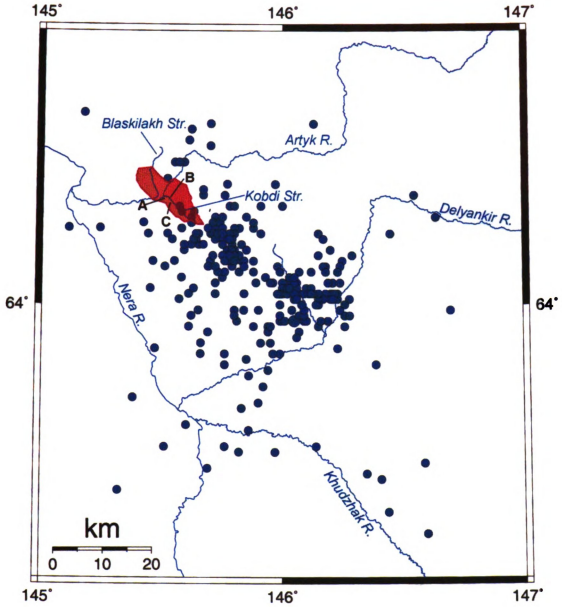

Figure 2-6. Area of mass movements, outlined in red, identified during field surveys after Artyk earthquake (Kurushin et al., 1976; Smirnov and Levashova, 1988).

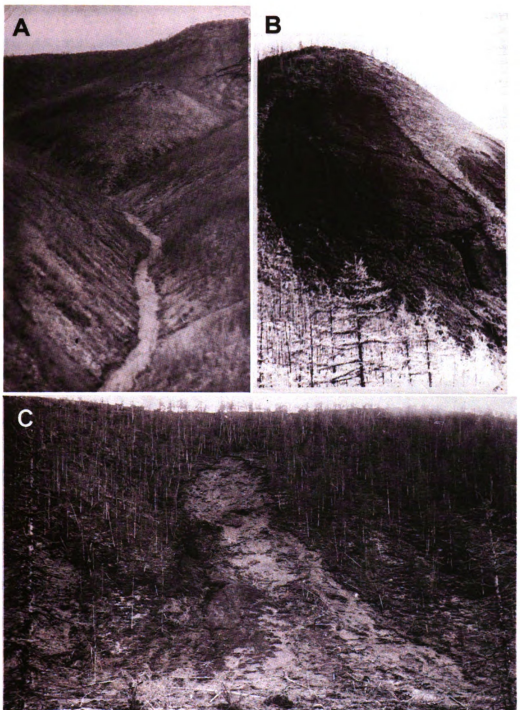

Figure 2-7. Photographs of ground failures and landslides from the Kobdi Stream valley referenced in figure 2-6 (photos courtesy of B.M. Koz'min).

most of the landslides were concentrated on the southwest side of Kobdi Stream, Kurushin et al. (1976) inferred that the rupture was located in the middle of the valley, rather than on the mapped fault location several kilometers to the northeast.

Subsequently, Smirnov and Levashova (1988) compared aerial photographs taken in 1957 and 1976 and satellite images taken in 1981 and identified additional landslides northeast of Kobdi stream and in the valley of the Blaskilakh stream on the north side of the Artyk River (Figure 2-6). This expands the area of landslides and other ground failures to about 90 km^2.

Kochetkov and Koz'min (1976) noted that the region of ground failures was offset from the epicenter by 15 km. They ascribed this difference to the dip of the fault plane and offset of the epicenter from the surface trace of the fault. It should be noted, however, that most of the ground failures occur in a topographically low region and that no failures are near the igneous intrusion forming the higher elevations closer to the epicenter. Thus, the lack of ground failures between the epicenter and the Kobdi Stream valley is likely simply due to ground conditions.

2.1.6 Aftershock Sequence and Temporary Deployment

Immediately after the mainshock, a series of aftershocks began to be recorded. Only one of the aftershocks (May 18, 1971 at 23:09:09 UTC) was recorded teleseismically.

At the time of the mainshock, the nearest permanent seismic station (see chapters 3 and 4) was Ust' Nera (UNR), operated by the Yakut network, approximately 150 km to the northwest of the epicenter. The second closest station was Susuman (SUUS), operated by the Magadan network, approximately 170 km southeast. Seimchan (SEY; Magadan network) was located about 350 km to the east of the Artyk event. No other stations operated within 500 km of the epicenter.

Following the mainshock and several significant aftershocks, the Yakut and Magadan networks deployed four temporary seismic stations within 50 km of the mainshock epicenter (Figure 2-8). The stations operated short-period vertical VEGIK seismometers with GB-III galvanometers with a magnification of about 15-20,000 (Kochetkov and Koz'min, 1976). Timing was by radio with automatic clock correction. The open and close dates were determined by examining the dates on which each station reported an arrival.

Table IV

Temporary Seismic Stations

Name	MSU Code	Latitude (°N)	Longitude (°E)	Elevation (m)	Open/Closed (1971)	Operator
Artyk	AYKS	64.18	145.13	700	6/3 – 7/31	YIGS
Kobdi	AY1S	64.20	145.51	800	6/8 – 7/13	YIGS
Ozernoe	AY2S	63.75	146.11	875	6/1 – 9/28	NEISRI
Tungussky	AY3S	64.20	146.38	1080	6/1 – 7/24	YIGS

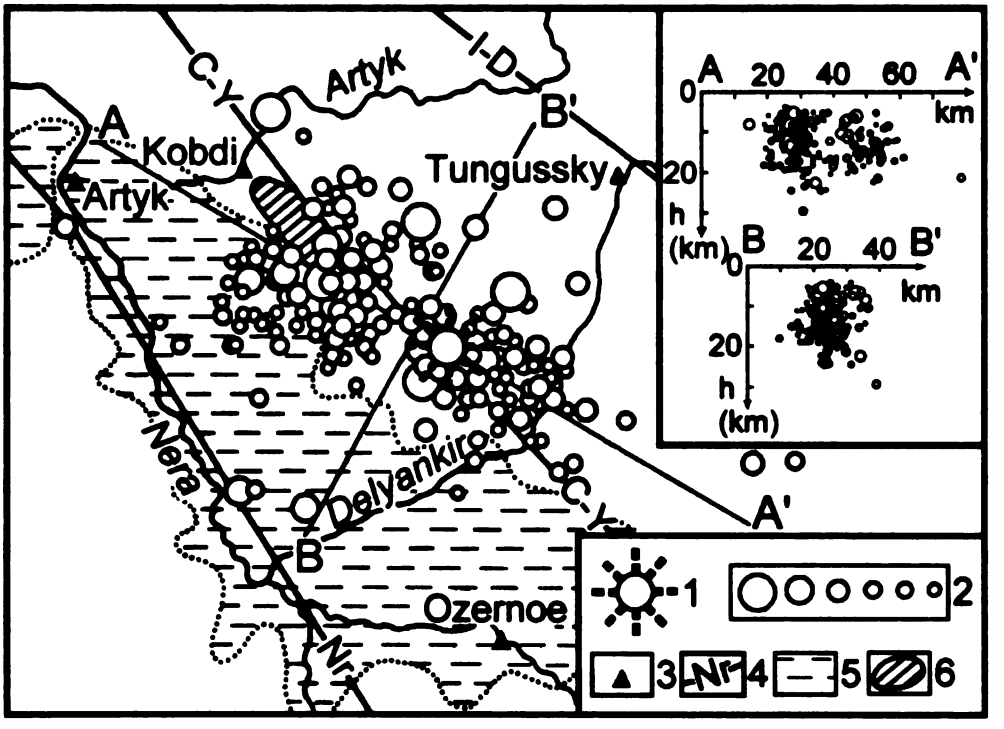

Figure 2-8. Distriubution of aftershocks of the Artyk earthquake as determined by the Yakut network. Inset shows cross sections of the aftershocks along lines parallel (A-A_1) and perpendicular (B-B_1) to the strike of the epicentral field (after Koz'min, 1984). 1 – Mainshock epicenter; 2 – Aftershocks, scaled by size; 3 – Temporary station; 4 – Faults; 5 – Upper Nera basin; 6 – Region of maximum ground failures.

Some 1,200 aftershocks were recorded during the course of 1971, of which about 500 were located (Figure 2-8) manually using intersecting arcs on paper. Kochetkov and Koz'min (1976) contend that the location error was less than 2 km for most events. They also calculated the focal depth for 212 events using x^2-t^2 relationships with a presumed error of ±5 km. The focal depths ranged from 2 to 29 km, with the majority being in the range of 10-18 km. The Yakut and Magadan networks worked cooperatively in the collection and analysis of data during the period of the Artyk aftershock sequence. The epicenters calculated by the Yakut network roughly paralleled the Chai-Yureya Fault (although somewhat different in strike) and vaguely defined a near vertical plane (Kochetkov and Koz'min, 1976; Koz'min, 1984).

K-class estimates, based on the methodology described in Rautian et al. (2007), for events during the aftershock sequence are between 6.5 and 13 (M approximately 1.5 to 5). Eleven of the aftershocks were larger than K-class 11 (M about 4; Koz'min et al., 1975), although only one of them occurred while the entire temporary network was operational (July 7, 1971).

The Russian-located events fall into two general clusters: one to the northwest of Mount Khulamrin and one to the southeast. Their main shock solution falls between the two clusters, with a fairly significant scatter of aftershocks (approximately 50 kilometer radius). Kochetkov and Koz'min (1976) contend that the aftershocks concentrated to the southeast in May and migrated to the northwest through the course of the summer of 1971.

In this thesis, I use the phase data from both the temporary and permanent stations to relocate the events using a better local travel-time curve and automated techniques (see chapter 4), and study the spatial and temporal distribution of the aftershock sequence and its relationship to the Chai-Yureya fault system (see section 2.2 and chapter 5).

2.2 Active Faults

Significant mapping of faults was conducted by Russian geologists through the 1980s under a pre-plate tectonics framework. Thrust faults, in particular, were not as commonly identified during this time frame. Following the collaboration of Russian and western scientists, a paradigm shift occurred that led to a greater understanding of the significance of many of the features that had been mapped (e.g., Parfenov, 1991; Parfenov and Kuz'min, 2001). The advent of satellite imagery and computer modeling has further dramatically changed our knowledge of large-scale tectonic features in northeast Russia.

One of the biggest questions currently associated with the seismicity of the CSB in general, and the Artyk sequence in particular, is the association of large earthquakes with mapped faults and their tectonic significance. This would be simple if faults were consistently mapped and published; however, the "mapping" of faults in northeast Russia and the interpretation of the

geology is a problem in and of itself, as it varies depending on what sources and references are utilized.

Russian scientists have mapped an extensive system of generally northwest-trending strike-slip faults throughout the CSB (Imaev et al., 1990, 1994, 2000; Gusev, 1979; Smirnov, 2000), but often place them in different locations or link them differently. These faults (Figure 1-3; e.g., Darpir, Ulakhan and the Chai-Yureya fault system) have been interpreted as the main seismogenic features in the CSB (Parfenov et al., 1988).

The Ulakhan fault system parallels the general trend of seismicity of the CSB and is thought to represent the primary present-day locus of displacement between North America and Eurasia, while the Chai-Yureya fault system is about 20-30° discordant to it and has been interpreted in various ways as noted in section 1.2.

2.2.1 The Ulakhan Fault System

The Ulakhan fault (Figure 1-3) is considered to be the largest fault in the CSB and perhaps in northeast Russia. It is clearly visible throughout its length in satellite imagery (Figure 2-9). It was initially identified by A. S. Simakov in 1949, and has been studied by many geologists (e.g., Imaev et al, 1990; Mal'kov, 1971; Gusev, 1979; Smirnov, 2000). Its status as the largest fault in the region is reflected in its name "Ulakhan," which translates as "great" in Yakutian.

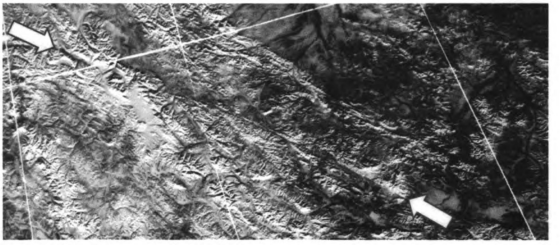

Figure 2-9. Russian "Meteor" satellite image showing the conspicuous Ulakhan fault (arrows). Courtesy B. M. Koz'min.

The Ulakhan fault has been traced by Russian workers from near the Indigirka River to the Seimchan-Buyunda basin, a distance of about 600 km (Figure 1-3; Imaev et al., 1990, 1994, 2000; Tret'yakov, 2003). Further northwest, the fault has been continued towards the Selennyakh or Yana rivers under various names, where it fades. To the southeast, the Ulakhan fault has been extrapolated from its visible termination near the southeastern edge of the Seimchan-Buyunda basin outward into the Sea of Okhotsk (Imaev et al., 1990, 1994, 2000). With these extensions, the total extent of this fault is over 1500 kilometers in length. The fault generally strikes northwest, with several releasing bends forming pull-apart basins, throughout its length (Imaev et al., 1990, 2000; Smirnov, 2000). Horizontal slickenlines are observed on the smooth surface of the fault (Imaev et al., 1990, 1994, 2000) and, combined with focal mechanisms of earthquakes, the fault is interpreted as being left-lateral (e.g., Fujita et al., in press).

The total horizontal offset on the Ulakhan has been estimated by Russian authors as 30-50 km, based on geology (Mal'kov, 1969, 1971; Imaev et al., 1994), and as 24 km along the entire trace of the Ulakhan based on offset rivers (McLean et al., 2000; Fujita et al., 2004, in press; Mackey et al., 2008b). Given that the river network is believed to have been established about 5 million years ago, this implies an average displacement of about 0.5 cm/yr (Fujita et al., in press), which is consistent with model calculations by Hindle et al. (2006) for various extrusion scenarios for the Okhotsk plate.

The Ulakhan fault proper is active with about 10-20 teleseismic events located within 10 km of it since the mid 1960s. The largest event was the October 19, 2006, event of magnitude Mw 5.2. The Ulakhan fault also marks the northern boundary of the zone of high seismicity in northeast Russia and is generally considered the northern edge of the Okhotsk plate (e.g., Parfenov et al., 1988; Riegel et al., 1993; Fujita et al., in press).

Multiple faults splay off or intersect the Ulakhan at an angle of about 30° at various points along its length. These include the Darpir, Chai-Yureya, In'yali-Debin (Umar), and other unnamed faults (Figure 2-10; Parfenov et al., 1988, Imaev et al., 1990, Smirnov, 2000) that cut across the highly seismoactive part of the CSB. Hindle et al. (in press) have suggested that these faults dissect and sliver the northern Okhotsk Plate.

2.2.2 The Chai-Yureya Fault

The Artyk earthquake is generally regarded as occurring on the Chai-Yureya fault (e.g., Koz'min, 1984). The Chai-Yureya fault, however, has been defined somewhat differently by different authors. The fault was first defined by B. I. Bronsky in 1936 and was initially mapped from the southern end of the Upper Nera Basin (Figure 2-11; section 2.3) to the Kolyma River at Orotuk (Figures 2-10, 2-11), continuing with a change in strike further southeast (Vashchilov, 1963; also unnamed but mapped on Larina, 1960).

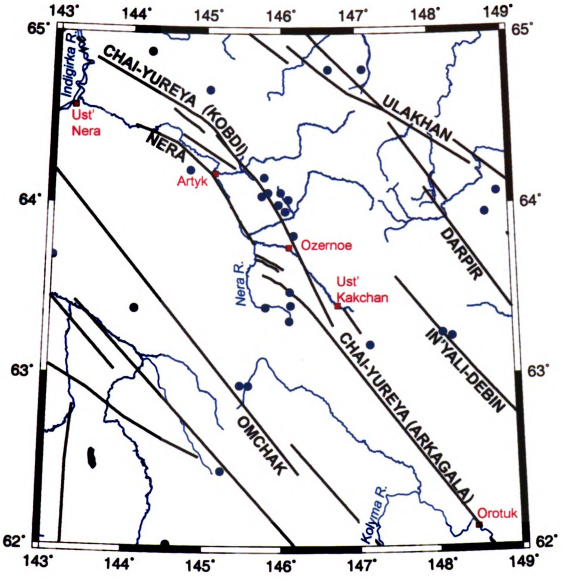

Figure 2-10. Teleseismic events that have been mapped in the vicinity of the Ulakhan and Kobdi faults. Relocated epicenters from MSU Database.

Subsequently, the Chai-Yureya has been extended by various authors (Imaev et al., 1990, 2000; Gusev, 1979; Smirnov, 2000) to both the northwest and southeast, resulting in a continuous proposed fault 600-700 km long between Ust' Nera on the northwest to the northeast of Magadan (Figure 1-3) in the southeast. The northern extension, from Ozernoe to Ust' Nera incorporates the Kobdi fault of Kurushin et al. (1976; see section 2.2.3). The southern extension is shown by a number of authors who extend the Chai-Yureya Fault further to the southeast to Atka (Gorodinsky, 1982; Korol'kov, 1992; Gusev, 1979; Imaev et al., 1990, 2000) or to the Yama River basin (Smirnov, 2000). Because the connections between the various fault sections are uncertain, we use the term "Kobdi Fault" for the section between Burustakh and the Delyankir River, "Arkagala Fault" refers to the well-mapped section between Ust' Kakchan and Orotuk (Figure 2-10), and "Chai-Yureya Fault" refers to the entire fault, including extensions, as used by Imaev et al. (2003; Figure 1-3).

2.2.3 Kobdi Fault

The Kobdi Fault (Figure 2-10; Kurushin et al., 1976), as mapped, extends from south of Mt. Khulamrin northeast to Burustakh (Fig. 2-1) along the northeastern edge of the Upper Nera basin (Fig. 2-11; Surmilova et al., 1986). The Kobdi Fault may continue further northwest (q.v., Shilo, 1961). Imaev et al.

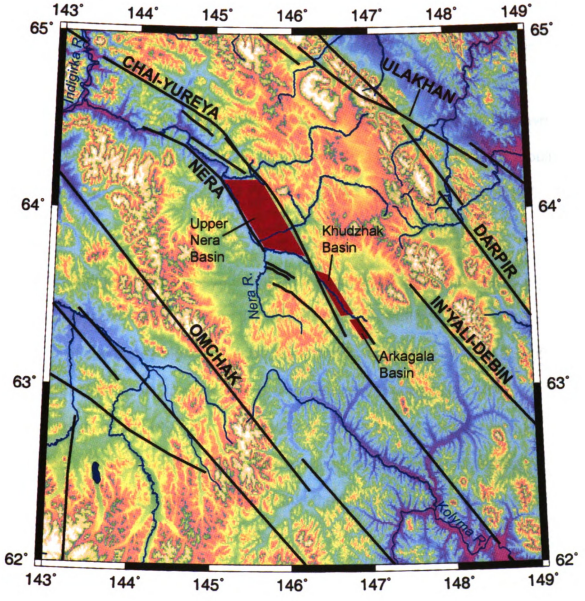

Figure 2-11. Generalized faults and geographic features in the Artyk earthquake area. Faults shown in black with black text. The Kobdi and Arkagala faults form the Chai-Yureya Fault. Basins are highlighted red.

(1990, 2000), Gusev (1979), and Koz'min (1984) consider the Kobdi Fault to be a continuation of the Arkagala Fault and bound the Upper Nera basin on the northeast (Figures 2-10, 2-11), with the Nera Fault (see section 2.2.5) possibly continuing the displacement of the Chai-Yureya Fault to the northwest towards Ust' Nera (Figure 2-11). In this model, the Upper Nera basin is a pull-apart basin due to the stepping of the Chai Yureya Fault (Imaev et al., 1990, 2000).

Investigations of the Kobdi Fault in the epicentral zone of the Artyk earthquake show slickenlines on the fault surface that indicate left-lateral motion. In exposures along the Artyk River and its tributaries on the edge of the Upper Nera basin, transtension is also observed (Imaev et al., 1990, 2000). Imaev et al. (1990) also note that the strike-slip character the fault is indicated by monotonic left-lateral "knee-shaped" bends in river channels in tributaries of the upper Nera River and that the fault is marked in higher relief by deep saddles and linear river valleys.

Analysis of satellite images and topographic maps suggests 1-4 km of left-lateral offset on some of the tributaries of the Nera River northwest of Mount Khulamrin (Figure 2-12). In addition, the Late Jurassic quartz-diorite and diorite intrusion that forms Mount Khulamrin appears to be divided into two parts offset by left-lateral motion of about 8 kilometers (Fujita et al., 2002).

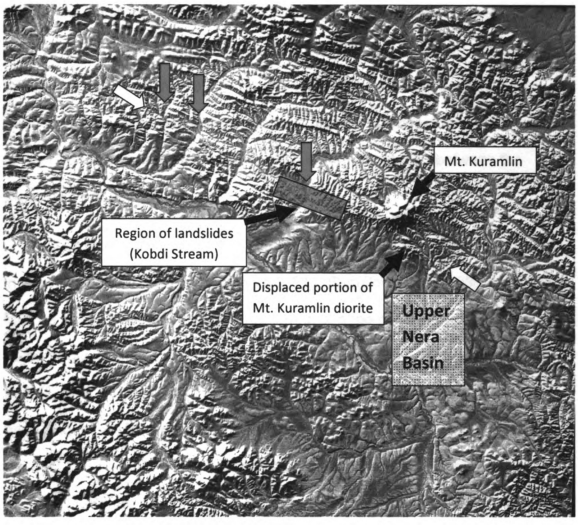

Figure 2-12. Satellite image of the Nera River basin showing proposed trace of the Kobdi Fault (white arrows) and the offset diorite of Mt. Khuramlin. Red arrows show possible left-lateral river offsets. Blue shaded area shows region with greatest number of landslides.

The Kobdi Fault between Mt. Khulamrin and Burustakh has been the most seismically active transecting fault in the CSB (Figures 2-10, 2- 14). Six teleseisms, including the 1971 Artyk event and one of its aftershocks, have been located in close proximity to this fault and an additional three epicenters to the northwest may be associated with it further northwest (between the Burustakh and Indigirka rivers).

The exact location of the Kobdi Fault varies between authors, especially in the vicinity of Mt. Khulamrin (Figure 2-13). Surmilova et al. (1986) map the fault as passing south of both Mt. Khulamrin and the offset part of the intrusion noted above (Figure 2-13a). Shilo (1961), who does not explicitly name the fault (Figure 2-13b), and Kurushin et al. (1976) map the fault between the two parts (Figure 2-13a). In addition, Shilo (1961) also shows a slight curvature to the east at the southern end of the Kobdi Fault. Imaev et al. (1990, 2000) and Koz'min (1984) do not distinguish the Kobdi Fault and refer to it as the Chai-Yureya Fault and consider them one and the same fault (Figures 2-10, 2-13b).

One significant discrepancy is the existence and nature of the connection between the Kobdi Fault and the Arkagala Fault. If they are continuous, a small restraining bend is required near Ozernoe; however a topographically low region is mapped instead as part of the Upper Nera or Khudzhakh basins. On face value, the curve in the trace of the Kobdi fault as mapped by Shilo (1961) would extend the Kobdi fault either into the fault segments in the west of the Khudzhakh basin (Figure 2-10) or curve it further

Figure 2-13a. Detailed fault map of the epicentral region of the Artyk earthquake showing the Larina (1960), and Surmilova (1976) and Kurushin et al. (1976) interpretations for the Kobdi and Arkagala faults.

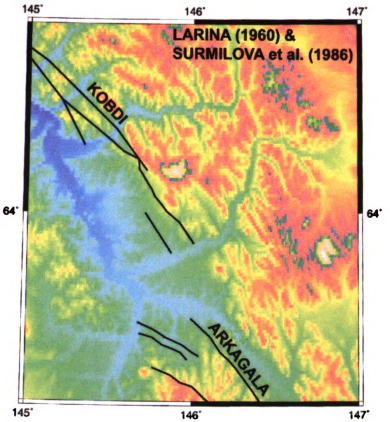
145°
146°
147°
LARINA (1960) &
SURMILOVA et al. (1986)
KOBDI
64°
ARKAGALA
145°
146°
147°

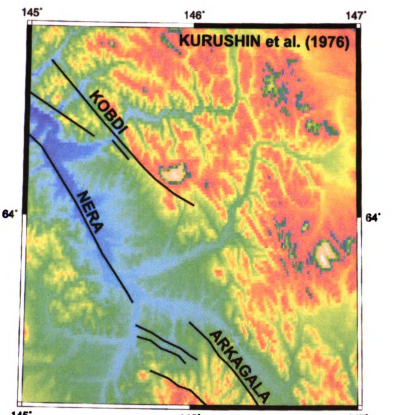
145°
146°
147°
KURUSHIN et al. (1976)
KOBDI
64°
NERA
ARKAGALA
145°
146°
147°

Figure 2-13b. Detailed fault map of the epicentral region of the Artyk earthquake showing the Shilo (1961) and Imaev et al. (2003) interpretations for the Kobdi and Arkagala faults.

SHILO (1961)
KOBDI
MELYANKIR
NERA
ARKAGALA
IMAEV et al. (2003)
CHAI-YUREYA
NERA
145°
146°
147°
64°

towards the In'yali-Debin (Umar) Fault (Figure 2-11).

2.2.4 Nera Fault

Koz'min (1984) suggests the presence of a fault that trends along the channel of the Nera River from Delyankir to Burustakh (Figures 2-1, 2-11, 2-13b) and continues in an arc along the southern edge of the Nera River valley to Ust' Nera (Imaev et al., 1990, 2000; Gusev, 1979) . The fault then defines the southeast edge of the Cenozoic deposits of the Upper Nera basin (see section 2.3).

Imaev et al. (1990, 2000, 2003) suggest that the Nera Fault steps and continues the displacement of the Chai-Yureya Fault to the northwest of the Upper Nera basin (section 2.3), thus interpreting the Upper Nera basin as a pull-apart basin stepping the displacement from the Nera Fault to the Kobdi Fault. They then connect the Kobdi and Arkagala faults by an arc to the southeast (Figure 2-13b). However, some mapped segments of the Arkagala Fault are roughly found along an extrapolation of the Nera Fault to the southeast and it is possible that the Nera fault is contiguous with the Arkagala fault.

The Nera fault is not particularly seismic although a few teleseisms have occurred along it during the instrumental period (Figure 2-10).

2.2.5 Arkagala Fault

The Arkagala Fault is clearly pronounced in the relief (Imaev et al., 1990, 2000) southeast of the Upper Nera Basin (Figure 2-11), especially where it has been exploited by the river network. The fault generally strikes 330°, and has a steep dip (Gusev et al., 1976; Gusev, 1979) of 70-75 degrees to the northeast (Smirnov, 2000).

The fault is traced as a series of en-echelon segments which form linear watershed divides and river valleys; there are a series of neotectonic scarps 300-600 m high (Smirnov, 2000). Multiple strands of the fault are mapped in a zone about 5 km wide (Larina, 1960; Gorodinsky, 1982; Gusev et al., 1976). It is also coincident with a chain of linear magnetic anomalies and a sharp step in the gravity field (Vashchilov, 1963). The amplitude of vertical displacement on the Arkagala Fault has been estimated as greater than 600-1000 meters (Gusev, 1979; Smirnov, 2000). There are no estimates of horizontal displacement, however, its present-day motion is interpreted as left-lateral (e.g., Imaev et al., 1990, 2000; Smirnov, 2000) based on offsets of tributaries of the Kolyma River (Imaev et al., 1990).

The Arkagala fault has been significantly less seismically active than the Kobdi fault and the level of activity is comparable to that of the Nera fault (Figure 2-10, 2-14).

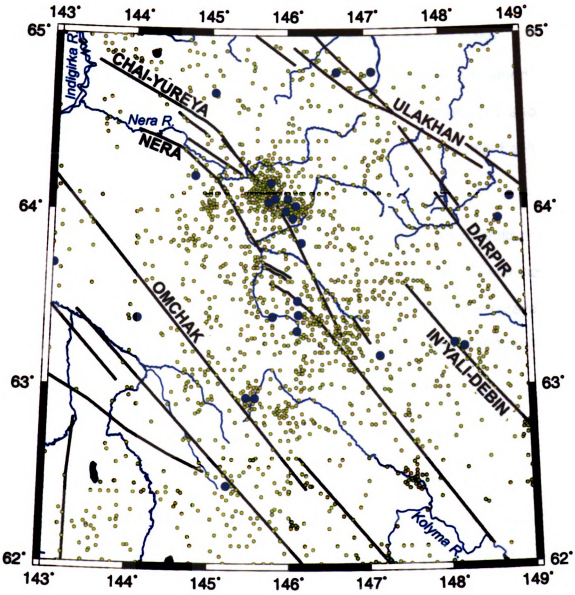

Figure 2-14. Detailed seismicity map of the epicentral region of the Artyk earthquake . Teleseisms shown as large, blue dots, microseismicity shown as small, green dots.

2.2.6 Other Faults and Lineaments in the Epicentral Zone

A number of other faults have been mapped or proposed in the epicentral region of the Artyk earthquake. Shilo (1961) maps an unnamed, southeast striking fault extending from Mt. Khulamrin for 15 km east of, and parallel to, the Mel'yankir River. We will refer to this as the Mel'yankir Fault (Figure 2-13b).

Shilo (1961) and Kurushin et al. (1976) also map a series of faults of southeast strike between the Khudzhak basin and the Inyali-Debin Fault that continue along the extrapolation of the Kobdi Fault, east of the Chai-Yureya fault system (Figure 2-11). The Inyali-Debin fault of Imaev et al. (1990, 2000) and Gusev (1970) is called the Umar Fault by Smirnov (2000).

2.3 Cenozoic Basins along the Kobdi, Nera, and Arkagala Faults

Numerous small Cenozoic basins are located along the Kobdi, Arkagala, and Nera faults (Figure 2-11). The Upper Nera basin is composed of Early Miocene and younger lacustrine and coarse clastic sediments (Shilo, 1961; Grinenko et al., 1998b) up to 615 m thick (Shilo, 1961). It is possible that some sediment deposits date as Paleogene in age (Shilo, 1961). The Late Cretaceous basement of the basins dips to the southwest (Kurushin et al., 1976).

Southeast of the Upper Nera basin is the Khudzhakh basin (Figure 2-11) of unknown age (Pleistocene?) with a visible sedimentary thickness of

50 m (Shilo, 1961). This basin is located in the transition zone between the Kobdi and Arkagala faults.

Farther southeast along Arkagala Fault are the Arkagala and other coal-bearing basins (Figure 2-11). Figures in Imaev et al. (1990, 2000) appear to interpret these basins as pull-apart basins, although they are older, Cretaceous, in age with a thin veneer of younger sediment superimposed on them (Cherepovsky, 1999).

Chapter 3: Artyk Seismological Database

The use of high-quality earthquake locations is important when seismicity patterns are analyzed to characterize the tectonics of a region. The MSU Northeast Siberian Seismicity database has significantly improved the seismological database for eastern Russia by integrating and using all available data - including international, regional and local data (see Mackey and Fujita, 1999, for details and sources). This, combined with improved velocity models and a standardized computer-based methodology for locating earthquakes, should greatly improve upon previous Russian hand-determined epicenters, especially when local stations are available.

3.1 Regional Networks

The Artyk region lies along the boundary between the spheres of responsibility of the Yakut and Magadan regional seismic networks (Figure 3-1). In the time period of the Artyk sequence, earthquakes were located by hand in both networks and were quantified according to the Russian K-class scale (q.v., Rautian et al., 2007).

3.1.1 Yakut Regional Network

During the Artyk aftershock sequence, the Yakutsk network operated 7 permanent stations (Figure 3-1).

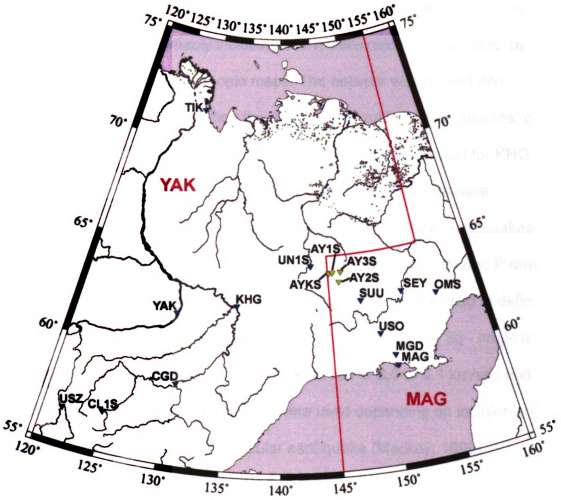

Figure 3-1. Permanent and temporary stations operating in northeast Russia during the Artyk aftershock sequence. Network boundary shown as red line; YAK refers to Yakutsk network; MAG refers to Magadan network. Permanent stations are represented as blue triangles. Temporary stations are represented by green triangles.

Throughout the analog era, earthquake locations determined by the Yakutsk network, presumably including 1971, were calculated by hand, by drawing arcs on 1:5,000,000 scale maps. The network was broken into northern (north of 60°N, including the Artyk region) and southern regions; only stations from one region were used in the location process except for KHG and YAK which were used in both regions. Epicentral distances were determined by Sg - Pg time differences for each station. Many earthquakes had phase arrival times from only three or four stations, and only one P arrival (usually Pg). In this case, the one available Sg - Pg time was used to define the origin time and other distances were determined using the Sg - origin time difference for the remaining stations. Pg velocities of 6.0 or 6.1 km/sec and Sg velocities between 3.5 and 3.7 km/sec were used depending on location and whichever "worked best" for a particular earthquake (Mackey, 1999).

3.1.2 Magadan Regional Network

During the time of the Artyk aftershock sequence, the Magadan district operated 6 permanent seismic stations (Figure 3-1). All stations operated at least one complete three-component set of instruments.

During the Artyk aftershock sequence, the Magadan network also used the arc on map method of drawing by hand (Mackey, 1999). The travel-time curve used was derived from the 1959 Magadan – Srednikan refraction profile (Davydova et al., 1968) with a three layer crust and calibrated for a hypocentral depth of 5 km. The uppermost layer is 6.0 km thick and has a Pg

velocity of 6.0 km/sec. The second layer is 14 km thick with a P* velocity of 6.7 km/sec. The third layer extends to 35.0 km depth and has a Pn velocity of 8.1 km/sec.

Mackey (1999) also notes that data listed in global databases, such as ISC, from both the Yakut and Magadan networks are preliminary time picks by station operators and often yield high residuals. This can be a result of poor time picks, Pg being reported as Pn, etc. In addition, historically, the Magadan network only had access to preliminary arrival picks from the Yakut network station UNR, thus UNR arrivals reported in the Magadan bulletin are sometimes different from that in the Yakut bulletin. The MSU Northeast Siberia database incorporates the final picks determined by network analysts.

3.2 Artyk Sequence Data

We collected phase data for all events of the Artyk sequence beginning on May 18, 1971 and ending September 6, 1971. This later date was used as the cut-off as earthquakes in the source region tapered off dramatically and fell outside of the expected rupture region after that time. In addition, the most of the temporary stations closed by the end of August, 1971. The data set was also restricted to a geographic area covering roughly 63 to 65°N and 145 to 147°E (an area of approximately 22,000 km^2). This area was defined by where the main cluster of aftershocks located, roughly equidistant around Mount Khulamrin (see section 2.4.6).

The mainshock and the first several weeks of aftershocks were recorded regionally only by the 13 operating permanent stations of the Yakut and Magadan regional networks. Phase data for the main shock and larger aftershocks were obtained from the MSU Northeast Siberia Seismicity data base which incorporates data from the International Seismological Center (ISC) on-line bulletin and *Byulleten' Zemletryasenii Sibiri 1971 g.* (*Bulletin of the Earthquakes of Siberia in 1971*; Golenetskii, 1973; hereafter *Byulleten'*. This publication is the predecessor to *Materialy po Seismichnost' SIbiri – Data on the Earthquakes of Siberia* – usually cited for more recent data).

Subsequently, as described in the previous chapter (section 2.4.6), the Yakut and Magadan regional networks deployed four temporary stations in the epicentral region of the Artyk earthquake to record the aftershock sequence. The phase arrivals for the temporary stations are not listed in *Byulleten'*.

The phase data in the MSU Northeast Siberia Seismicity database were then supplemented by phase arrivals at the stations of the Magadan network and the temporary station at Ozernoe (AY2S) obtained from the unpublished *Byulleten' Aftershokov Artykskogo Zemletryaseniya 18 Maya 1971 g.* (*Bulletin of the Aftershocks of the Earthquake of May 18, 1971*) produced by the Magadan network. This bulletin is composed of three parts covering different time periods: May 18 – June 10, 1971; June 11 – July 31, 1971; and August 1 – December 31, 1971. Two versions of the bulletin for the May 18 – June 10 period exist. The phase arrival times are the same in the two versions, but

they differ in how amplitudes are calculated. One of the versions also includes K-class determinations for the events while the other does not. These data were typed into the MSU database format. Epicenters were taken from *Byulleten'*, with a precision of 0.1 or 0.01 degree except for the events recorded in July which were taken from a list provided by Dr. Koz'min with a similar precision.

The resultant files were sent to Yakutsk where Dr. Boris Koz'min kindly entered the arrival times from the Yakut network stations (both temporary and permanent) through August 31, 1971 (only Ozernoe operated past this date). The data from Dr. Koz'min for May and June, 1971, were the same as in *Byulleten'*. For month of July, 119 events were new or had new phase data and 18 events for August were new or had new phase data. Data for 86 events were received from Dr. Koz'min that were not associated with a previously located earthquake and had no listed epicenters.

In general, there were no major discrepancies between the Yakut and Magadan data; however, the combined file was examined for inconsistencies and errors in October, 2002. Several specific problems were identified (see below) and sent back to Dr. Koz'min for further verification. A revised set of data was received in late November, 2002. These data were supplemented by phase data for 18 events from Seimchan (SEY) which the author obtained during a trip to northeast Russia in the summer of 2001.

The initial data set of 146 events (mainly from Magadan aftershock bulletin and *Byulleten'*) increased to 416 events with additional data from Dr. Koz'min, and the new picks from SEY.

The merging of the Yakut and Magadan data for their Artyk deployment did encounter some difficulties. Dr. Koz'min indicated that there were some interpretation or time problems with the data from June 1 through June 21. In particular, data listed as AY2S (Ozernoe) in the data from Dr. Koz'min were different than that reported in the Magadan aftershock bulletin and turned out in some cases to actually be AY1S. In those instances, the Magadan network data for AY2S were used, if available, as they were the operator of AY2S. Otherwise, arrivals for that station were omitted during that time frame. SUUS was also sometimes double listed with MAG listing a phase as SG and YAK listing the same phase as S. These and similar conflicts were resolved as best possible, however, they remain a possible source for some error.

Chapter 4: Data Analysis

This chapter discusses the methodology used in locating the aftershocks, post-processing quality filtering, and additional steps taken to understand the accuracy of earthquake locations used in this study.

Many multi-event relocation techniques (e.g., master event techniques, joint hypocenter determination, etc.) have been developed to improve relative locations within earthquake sequences. Such techniques depend on having at least one well located event with stations common to other events or relatively stable data sets with consistent and well distributed stations between the events (e.g., Douglas, 1967; Spence, 1980; Pujol, 2000). Because of the variability in station coverage and potential quality problems associated with the Artyk data set, as outlined in Chapter 3, we used a single-event procedure to determine the quality of the Artyk aftershock data set and to see if epicentral locations could be improved.

4.1 Crustal Velocities and Travel-Time Curves

Northeast Russia is a very large area undergoing complicated deformation, and was formed through the accretion of terranes of various crustal affinities (see introduction; e.g., Parfenov, 1991; Nokleberg et al., 2000; Parfenov and Kuz'min, 2001). Thus, a single or simplified velocity model for the entire region, as was used in previous Russian studies, is unlikely to represent the local crustal velocity within a specific part of the region.

In order to better determine a spatially varying travel-time curve for northeast Russia, Mackey (1999) subdivided northeast Russia into cells 3-degrees north-south by 5 degrees east-west. In each cell, events with 2 or more Pn phase arrivals were selected, which includes only the larger events which are recorded at more stations with a better azimuthal coverage. These events were then relocated using Pg velocities between 5.875 km/sec and 6.350 km/sec in increments of 0.025 km/sec and Sg velocities ranging from 3.47 to 3.65 km in 0.02 km/sec increments. For each velocity combination, the sum of the root-mean-squared (RMS) residuals for all events was calculated. The Pg and Sg velocity combination yielding the lowest sum was selected as the best-fitting velocity model for each cell.

Travel-time curves for both Pg and Sg phases were calculated using a flat-earth, straight-ray assumption since both of these phases are confined to the crust, thus the surface distance is roughly equivalent to the linear distance between epicenter and station.

For the region of the Artyk aftershock sequence, the best fit velocity based on 103 events was determined to be Pg = 6.025 km/sec and Sg = 3.510 km/sec (Mackey, 1999). Mackey (1999) also determined that the Jeffreys and Bullen (1940) travel-time curves for Pn and P yielded better locations than the IASPEI 1991 curve of Kennett (1991). Thus, these velocities and the travel-time curves were used in the relocations in this thesis.

Steck et al. (2009) obtained Pg = 5.99 km/sec and Sg = 3.487 km/sec in a recent tomographic study.

4.2 Location Procedure

In this study, we used a standard, least squares, best fit hypocenter location program modified by K. G. Mackey to accommodate multiple travel-time curves and phases, specifically Pg, Pn and Sg. Sn phases were not used because they were considered too noisy in the Northeast Siberian dataset (Mackey, 1999). The program iteratively solves for improved hypocentral and origin time estimates. Following an iteration of the program, the previous solution becomes the new starting value for the location program. A total of five iterations are completed during which the change in the RMS residual decreases to some desired value acceptable to the operator of the program.

The aftershock sequence consists of 1,200 earthquakes, of which approximately 500 were hand located by the Russian networks (Figure 2-8). Of these, 416 were selected to be located using the computer algorithm. The Russian determined epicenters obtained from the *Byulleten'* and Dr. Koz'min (section 3.2) were used as the initial estimate for origin time, location and focal depth. The travel-time curves used were discussed in section 4.1.

4.2.1 Removal of High-Residual Stations

Following an initial relocation, each event RMS residual was examined. In general, event residuals below ±1.5 sec were initially considered

acceptable. If a first pass did not yield convergence of the routine to an acceptable mean residual, individual outlying phase arrivals were removed and the epicenter was recalculated. Following the initial relocation of the earthquakes, stations with an individual arrival residual of greater than ±3.2 seconds were eliminated. Some arrivals with lower, but significant, residuals were also removed if the station was very close to the epicenter (for example, the temporary network stations) and/or if a single residual had a value several times larger than all others for a particular event. Final event residuals were typically below ±1.0 second. In general, higher event RMS residuals were associated with events that had a higher number of reporting stations and arrivals, or with stations that were a considerable distance from the epicenter.

After the initial relocation pass, 407 events were retained. The events that were removed from the data set either relocated to a location significantly outside of the study area (and therefore were not considered associated with the aftershock sequence) or they did not converge to a stable value regardless of the removal of outlying arrivals. Of the 407 events, 121 events retained arrivals from three or fewer stations and were not used in further analysis. 286 events had four or more stations and were included in the final results .

4.2.2 Impact of Individual Stations

The Artyk aftershock data set is unique for the study area in that there was considerable station coverage, both local and regional, which allowed the opportunity to assess the impact of individual stations on earthquake locations.

It is expected that the greater the number of stations and defining phases, and the smaller the azimuth gap between stations around an earthquake, will result in a better quality location. Due to the extensive amount of faulting in the area, location accuracy needs to be within a few kilometers to be able to associate earthquakes to specific faults. The complicated geology combined with the relatively low number of seismic stations operating in the area means that an individual station could significantly bias an earthquake location.

4.2.2.1 Regional Stations (General)

An experiment was performed to determine the impact of removing selected regional stations' arrivals used in event relocations. Several events were evaluated with different combinations of regional coverage (Figure 4-1).

One aftershock (May 18, 1971, at 23:09:09 UTC) had both regional and teleseismic stations reporting (7 regional, 12 teleseismic). The largest azimuth gap between all stations was 90° (but between regional stations was between 90 and 180). For this event, the effect of removing one regional station out of the location process was minor (an average of 1.57 km when the teleseismic stations were also included; 1.67 km without). As expected, the effect of removing a regional station was more significant if multiple phases were reported and if the station was closer to the epicenter. OMS is the only regional station for this event in which P, PG and SG phases are available. Removing it moved the location 2.89 kilometers (1.7 km if the teleseismic

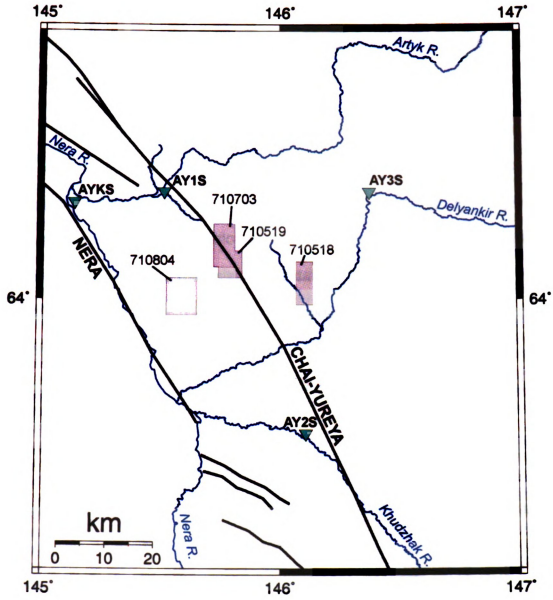

Figure 4-1: Overview showing locations of epicenter location experiments. Inverted triangles represent temporary stations. Faults after Imaev et al. (2003) shown as black lines.

stations were included). Another observation of this experiment is that locations using teleseismic stations plotted more to the north; with just the regional stations, they mapped more to the south and east (Figure 4-2).

For events where station coverage was less robust, with no teleseismic coverage, but still fairly decent regional coverage and a moderate azimuthal gap (greater than 90 and less than 180 degrees), the effect of removing one regional station out of the location process actually moved the location less, on average, than the event with teleseismic data. For example, for the event May 19, 1971 at 03:16:31, with 7 stations (all regional) the effect of removing one regional station moved the location about 1.35 kilometers on average. Removing station UN1S was most significant, with location difference of 2.43 kilometers (Figure 4-3).

Comparing the effect of regional stations with that of the temporary network is also useful. An example of an event with decent regional and local station coverage is the July 3, 1971 event at 06:51:59. There were three temporary stations reporting during this event AY1S, AYKS, AY3S. Removing any of the temporary stations moved the location about 0.72 kilometers on average. Removing any of the regional stations (UN1S, SUUS, SEY or USO) moved the location about 1.20 km, on average; if the temporary stations were also reporting, the location moved an average 1.0 km (Figure 4-4). Note that SUUS has a significant effect, ahtough still only about 5.6 km (see section 4.2.2.2).

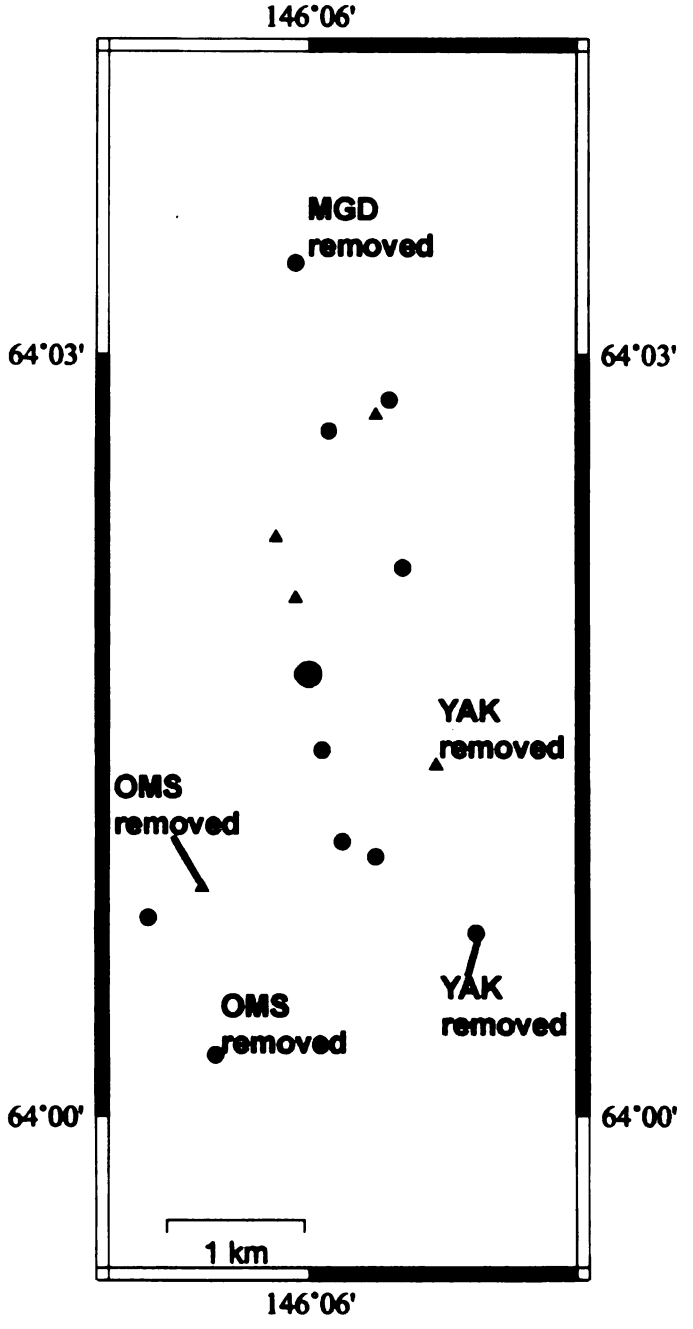

Figure 4-2. Event of May 18, 1971, 23:09:09 UTC. Relocation is represented by a large, red circle. Yellow triangles represent epicenters for which regional and teleseismic arrivals used in the calculation; blue circles are where only regional arrivals were used in the calculation. For both, regional station arrivals were removed from the calculation on a station by station basis (the station that was removed is noted when significant).

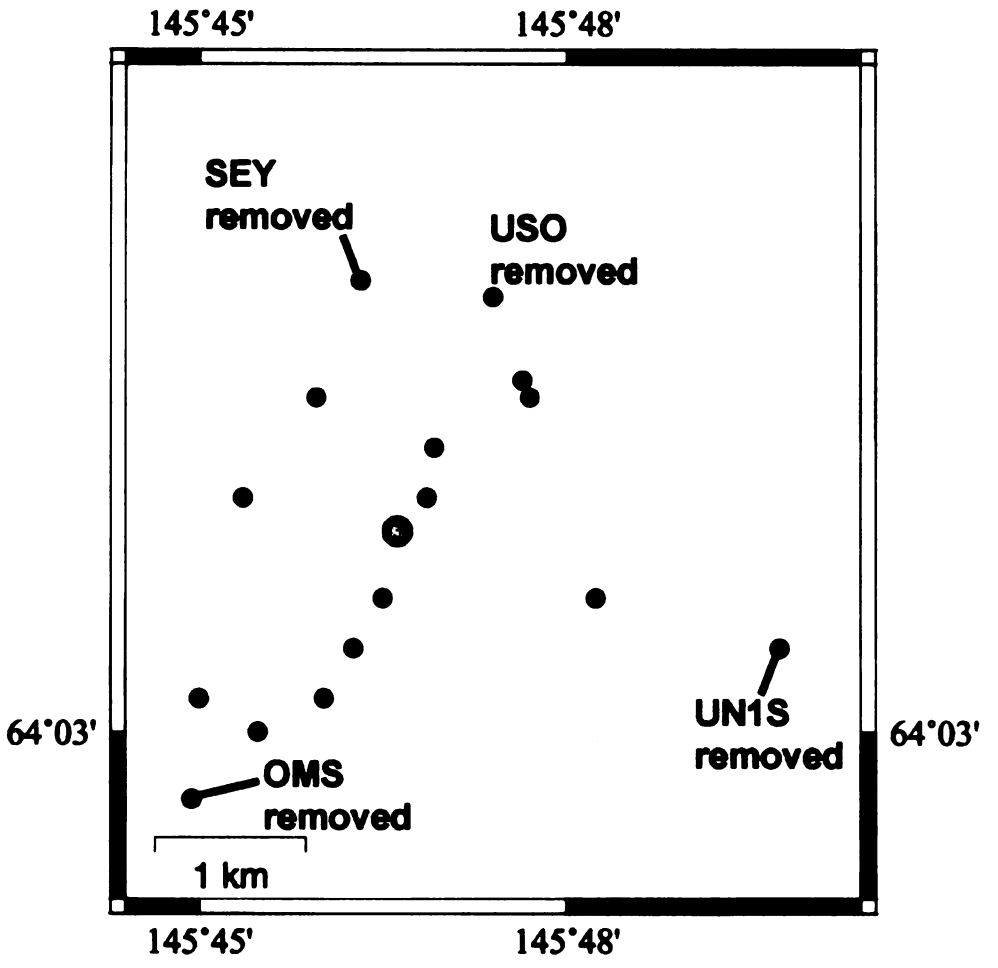

Figure 4-3. Event of May 19, 1971 at 03:16:31 UTC. Relocated epicenter calculation using all stations is represented by a large, red circle. Blue circles are events for which station arrivals (regional, temporary) were removed from the calculation on a station by station basis (the station that was removed is noted when significant).

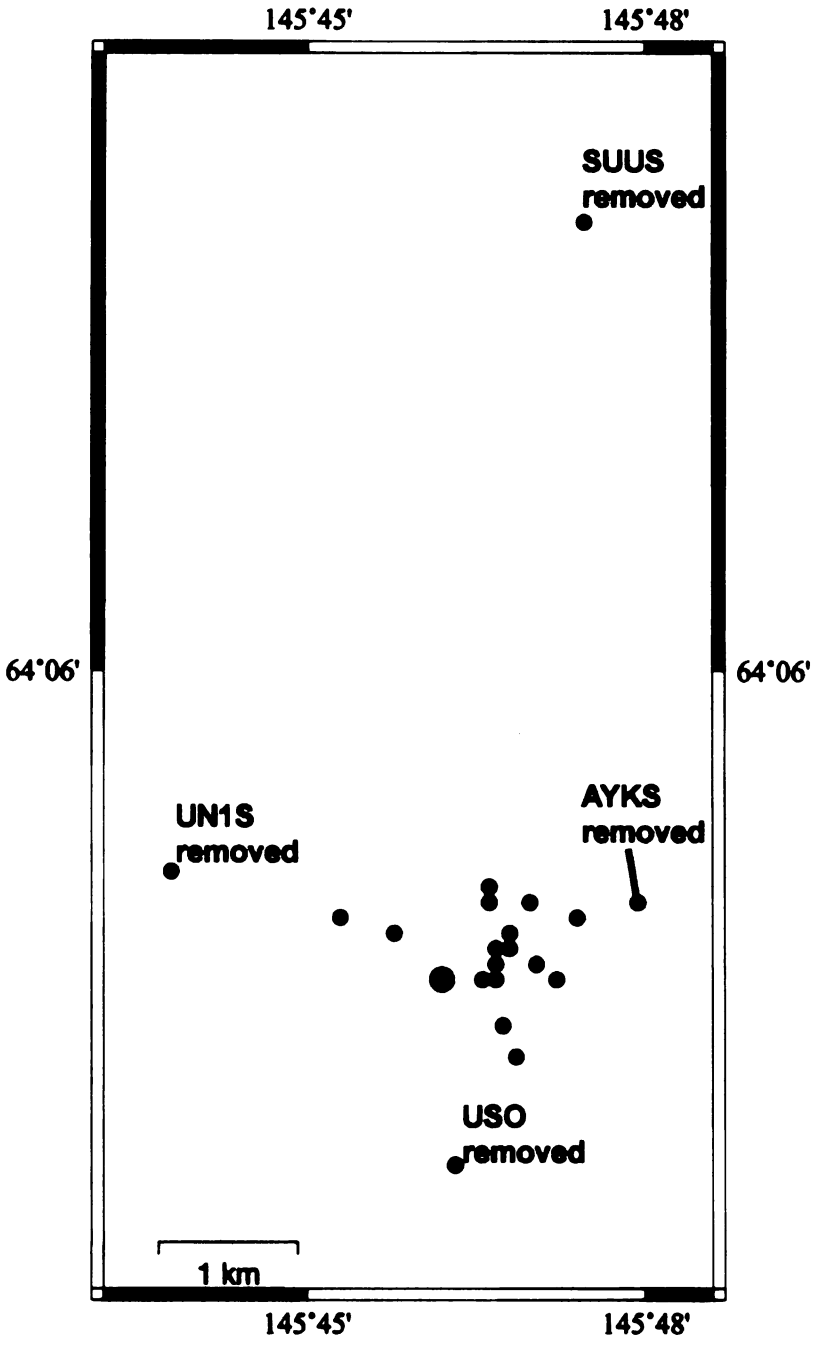

Figure 4-4. Event of July 3, 1971 at 06:51:59 UTC. Relocated epicenter calculation using all stations is represented by a large, red circle. Blue circles are events for which station arrivals (regional, temporary) were removed from the calculation on a station by station basis (the station that was removed is noted when significant).

Another example of an event with considerable regional station coverage (10 stations) is the August 4, 1971 event at 02:11:47. There was one temporary station reporting during this event (AY2S), which had a minor effect on the location (removing it only moved the location 0.98 km). The effect of removing one regional station moved the location about 1.64 kilometers on average. The effect of removing SEY was most significant, which moved the location approximately 5.2 kilometers (Figure 4-5).

4.2.2.2 Specific Stations

When assessing the distribution of the Artyk aftershocks, it became apparent that certain individual stations (e.g. UN1S, SUUS) were more significant in influencing the location of an earthquake than others. For events which had both stations UN1S and SUUS reporting, locations were observed to move significantly when one or the other station was not used. In general, however, the locations moved less than 6 kilometers when one or the other station was removed.

To assess how significant this might be, I plotted events from June through early July for which both UN1S and SUUS reported arrivals. We chose this time period because it was the time period of maximum coverage from regional and local stations. Events were relocated with one of the two stations removed and compared to the location with both stations reporting. Events which had only UN1S reporting were an average of 3.5 km offset to the northwest; those with only SUUS reporting were an average of 2.0 km offset to

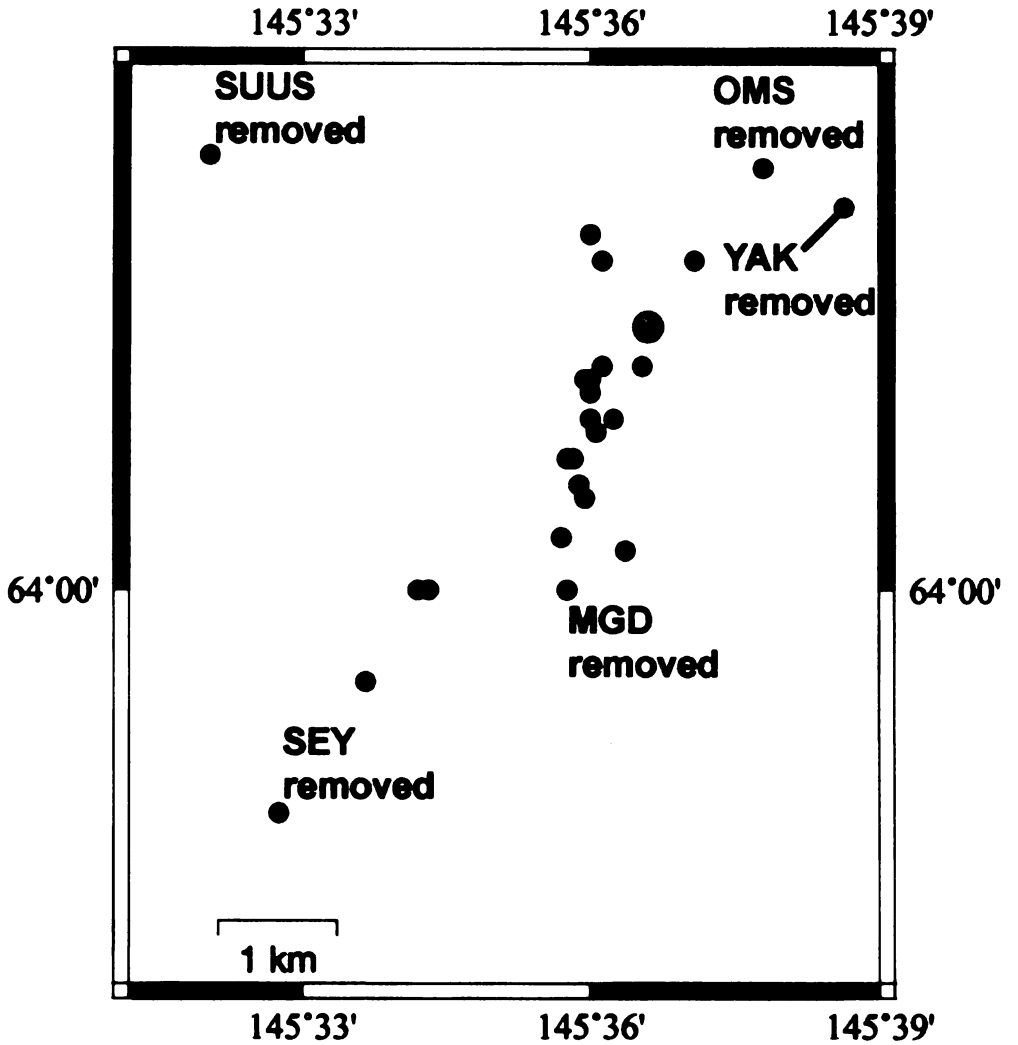

Figure 4-5. Event of August 4, 1971 at 02:11:47 UTC. Relocated epicenter calculation using all stations is represented by a large, red circle. Blue circles are events for which station arrivals (regional, temporary) were removed from the calculation on a station by station basis (the station that was removed is noted when significant).

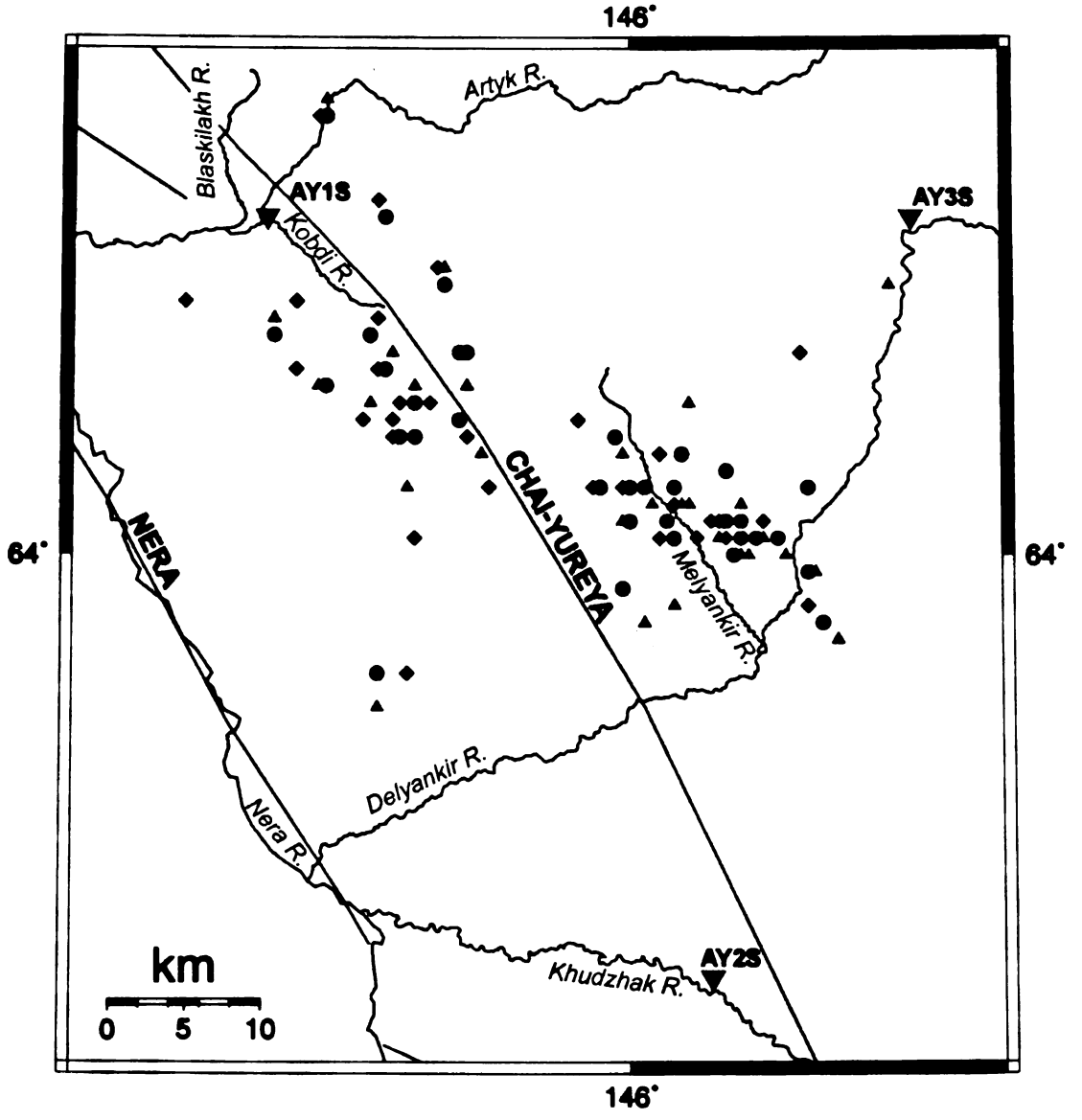

Fig. 4-6: Plot of June and early July locations which had stations UN1S and SUUS reporting. Inverted triangles represent temporary stations. Green circles are the locations calculated with both stations; red triangles are locations calculated with station SUUS removed; blue diamonds are locations calculated with station UN1S removed. Faults after Imaev et al. (2003) shown as black lines.

the southeast. The locations were offset from each other by an average of 3.8 km, the difference generally oriented northwest-southeast; the distribution and general location of the events, however, does not substantially change (Figure 4-6).

4.3 Location Quality

Previous studies (e.g., Yang et al., 2000) have suggested that the confidence in epicentral location accuracy is dependent on the number of stations within a particular distance from the epicenter and the largest azimuthal gap between recording stations. For this study, we developed criteria to estimate the quality of the event locations that we use to associate earthquakes to specific faults. Three quality groups were created, based on the number of stations reporting and the largest azimuth gap between stations. The criteria are summarized in Table V:

Table V

Quality Criteria Used in this Study

Quality Group	Number of Stations	Largest Azimuth Gap
		(degrees)
1	6+	Less than 180
2	5	Less than 180
3	4	Less than 180
	Any	Greater than 180

Relocated events are plotted based on these quality categories.

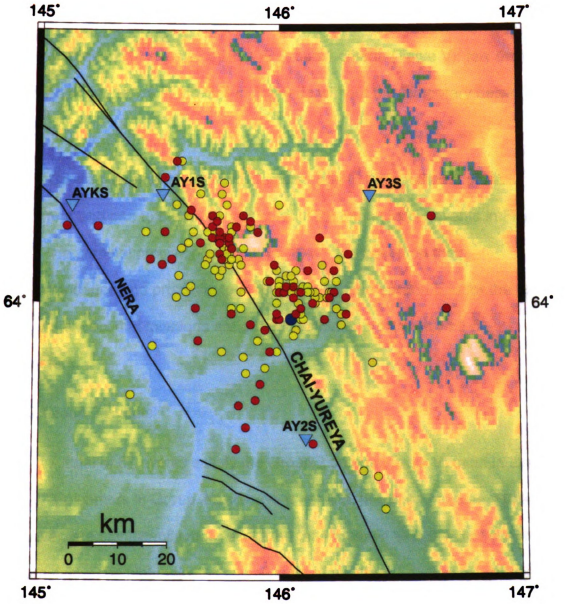

Figure 4-7: Mainshock (blue), group 1 (yellow) and group 2 (red) quality categories events on Imaev et al. (2003) mapped faults. Inverted triangles represent temporary stations.

4.3.1 Group 1 Events

A total of 114 events satisfy the Group 1 criteria (Table V); few events in the Artyk sequence fit the Group 1 criteria without the temporary network stations.

Group 1 events fall into two clusters: one to the southeast of Mt. Khulamrin and one to the northwest of Mt. Khulamrin (yellow events in Figure 4-7). The nominal precision is about ±5-10 km but based on their correspondence and proximity to mapped faults (see section 5.1) for the most part, we expect that locations are good to within approximately ±3-5 kilometers.

4.3.2 Group 2 Events

A total of 67 events satisfy the Group 2 criteria (Table V) used in this study. Epicenters in Group 2 also have a nominal precision of about ±10 km, however, are significantly more scattered than those in Group 1 (red events in Figure 4-7). The plot indicates two clusters of events, as in Group 1, although earthquakes fall a greater distance from the mapped faults (see section 5.1).

4.3.3 Group 3 Events

Group 3 events can either be recorded by at least 4 stations, with the largest azimuthal gap between reporting stations of less than 180°, or recorded by any number of stations but with the largest azimuth gap between

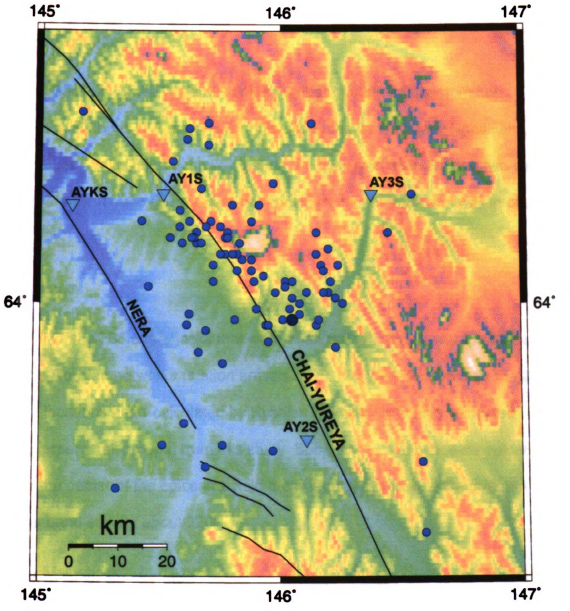

Figure 4-8: Mainshock (blue), group 3 (light blue) quality categories events on Imaev et al. (2003) mapped faults. Inverted triangles represent temporary stations.

reporting stations being greater than 180°. A total of 103 events fell into the Group 3 criteria.

Because of the generally small number of stations, the nominal precision is about ±7 km; however, the Group 3 events show a significant amount of scatter, although two clusters are observed as in the first two cases (Figure 4-8). These events were not considered in the fault analysis in chapter 5.

4.4 Results

Of the 286 aftershocks that were analyzed, 45 events were not located by the Russian networks (station arrivals only). Figure 4-9 compares the 241 initial locations hand-calculated by Russian networks with their relocated counterparts (all groups) from this study. Subjectively, the relocated epicenters near the center of the epicentral field are more tightly clustered and form a linear band striking about 320°.

4.4.1 Mainshock

The relocated Artyk mainshock is south of Mt. Khulamrin at the southeast end of the aftershocks (Figure 4-8), consistent with the event rupturing to the northwest as determined by directivity studies of Filson and Frasier (1972). The previous Russian locations place the main shock about 20 km to the northwest of the relocation, within the center of the aftershock sequence (Figure 2-2; Table I; Kochetkov and Koz'min, 1976; Koz'min, 1984).

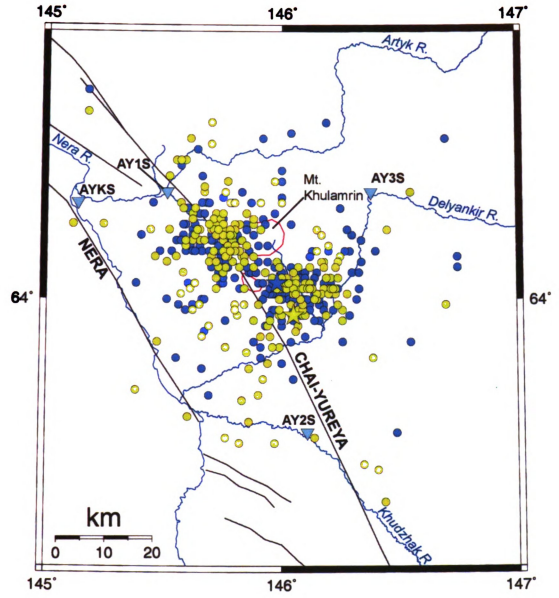

Figure 4-9: Comparison of the Russian original (blue) and relocated (green) epicenters. Inverted triangles represent temporary stations. Faults after Imaev et al. (2003) shown as black lines.

Comparison of the relocated mainshock epicenter (Table I) to previously determined solutions yields some systematic differences. The Russian solutions (Yakut network solutions, Obninsk, Kondorskaya and Shebalin, 1977) generally tend to fall to the north and northeast of my relocated epicenter.

Western teleseismic solutions (NEIC, ISC, Engdahl et al., 1998) tend to fall to the south and southeast, less than 10 kilometers from the relocation. The mainshock relocation from this study differs insignificantly from that reported in Mackey and Fujita (2001).

4.4.2 Aftershocks

The better quality (groups 1 and 2) relocated aftershocks, much like the original Russian locations, plot in two clusters (section 2.4.6; Figure 4-7). One is northwest of Mt. Khulamrin, the other is southeast. The relocations, however, line up much more tightly and curve slightly more to the southeast south of Mt. Khuramlin (see section 5.1). There is still some scatter in the relocations and some events continue to locate in the Nera basin. Relocated epicenters moved, on average, approximately 11.2 km. The largest distance between original and relocated epicenters was about 70 km; the largest changes appear to occur during the time the local network was not operating.

The scatter of aftershock relocations varies greatly between three general time periods: May (when there were no temporary local stations),

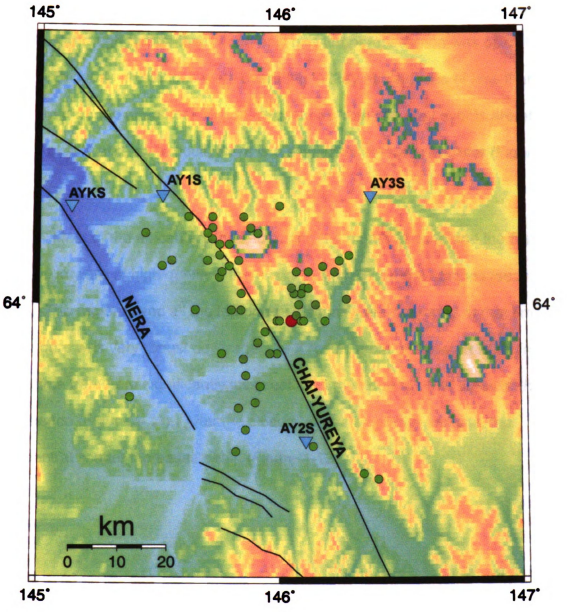

Figure 4-10. Epicenters from the month of May. Main shock represented as large, red circle. There were no temporary local stations (inverted triangles) operating during this time period. Faults after Imaev et al. (2003) shown as black lines.

June through early July (when all four temporary stations were operating), and late July through September (when only one temporary station was operating).

Because no stations were operating in May at distances of less than 150 km from the aftershock region, relocations from late May events are of lower quality and, as a result, there is a significant amount of scatter (Figure 4-10).

Most of the epicenters located during the month of June and the first half of July are of high quality if there is data from 6 or more stations (section 4.3). The regional and all the temporary stations were operating at that time, and there was very robust coverage. As a result, most of the epicenters from that time frame are significantly less scattered than during other times of the sequence (Figure 4-11). After the closure of the temporary stations, the epicentral scatter increases again (Figure 4-12).

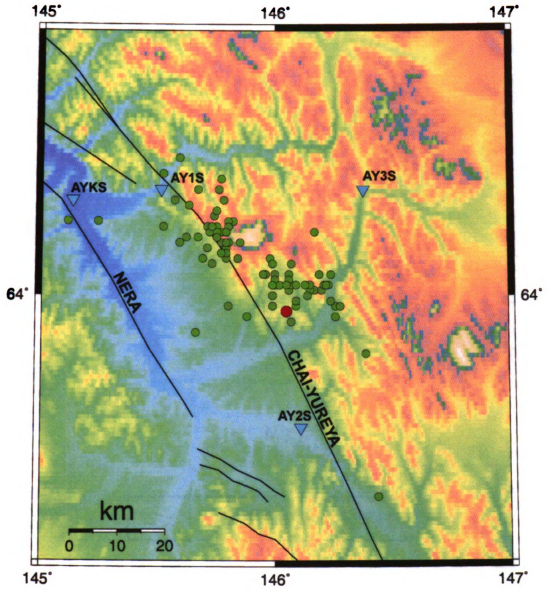

Figure 4-11. Epicenters from the first of June through early July. Main shock represented as large, red circle. Regional and local temporary stations (inverted triangles) were operating during this time period. Faults after Imaev et al. (2003) shown as black lines.

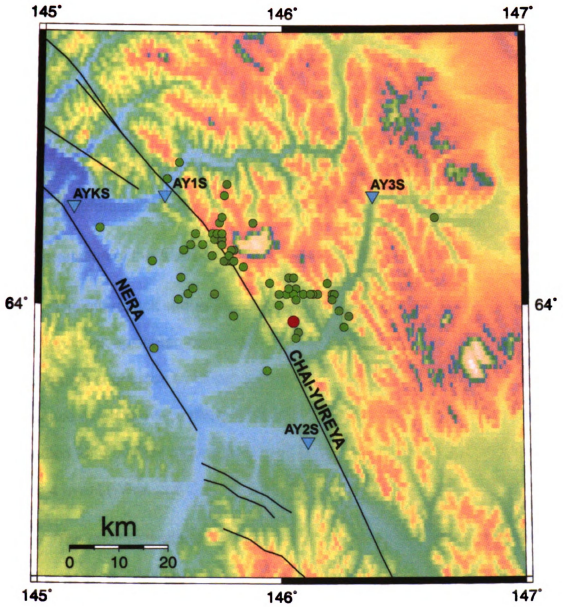

Figure 4-12. Epicenters from late July through the end of August. Main shock represented as large, red circle. Only regional stations were operating during this time period. Temporary stations represented as inverted triangles. Faults after Imaev et al. (2003) shown as black lines.

Chapter 5: Discussion

The relocated earthquakes from the Artyk aftershock sequence were examined in terms of their temporal and spatial distribution, their relationship with mapped faults and lineaments visible on satellite imagery and maps, and with macroseismic data. These observations are used to speculate about the nature of deformation in the northern Okhotsk plate.

5.1 Correlation of the Aftershocks with Mapped Faults

The aftershock sequence relocates, in general, north and northwest of the mainshock epicenter, consistent with the northwesterly rupture propagation suggested by Filson and Frasier (1972). The aftershock sequence extends over a distance of approximately 25-30 km, roughly that expected for a surface rupture from the empirical scaling relationships for a Mw 6.4 event (Wells and Coppersmith, 1994).

The relocated aftershocks generally form a linear trend in the cluster northwest of Mt. Khulamrin with an approximate strike of 315-320° (Figure 5-1). This strike is consistent with one of the nodal planes of the mainshock focal mechanism (314°; section 2.1.3).

To determine which proposed local fault mapping is most consistent with the aftershock data, I compared the relocated epicenters to the four variant mapping of faults in the Mt. Khulamrin area that have been proposed:

Figure 5-1a. Relocated epicenters (blue dots) superimposed on top of faults as mapped by Larina (1960) and Surmilova et al. (1986), and by Kurushin et al. (1976).

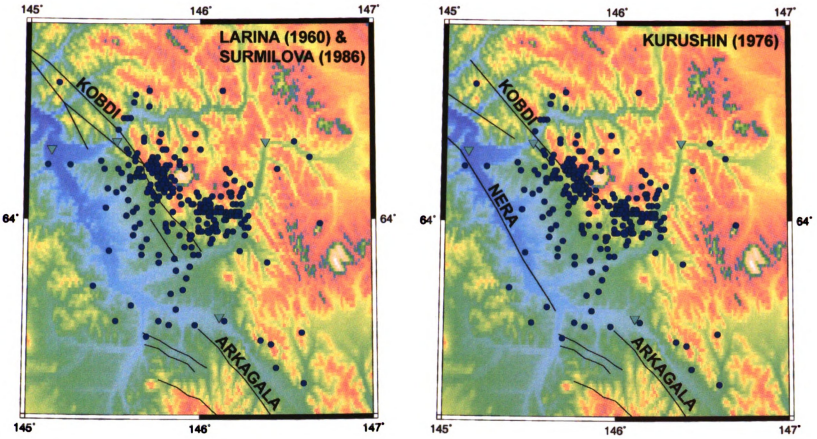
LARINA (1960) &
SURMILOVA (1986)
KOBDI
ARKAGALA
KURUSHIN (1976)
KOBDI
NERA
ARKAGALA
145°
146°
147°
64°

Figure 5-1b. Relocated epicenters (blue dots) superimposed on top of faults as mapped by Shilo (1961) and by Imaev et al. (2003).

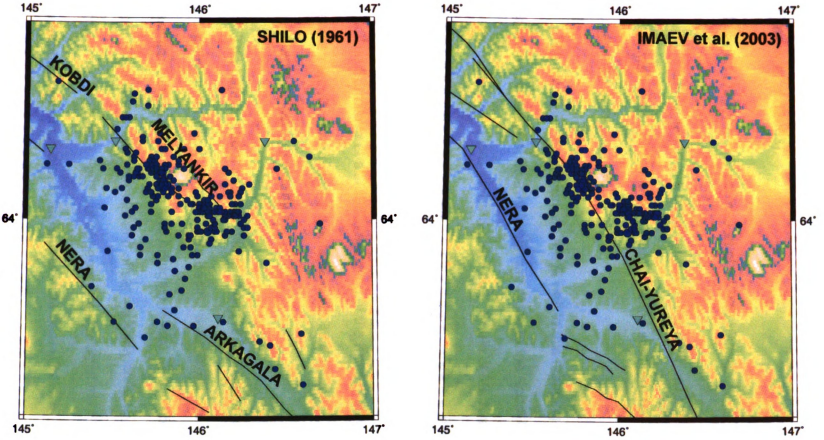
SHILO (1961)
KOBDI
MELYANKIR
NERA
ARKAGALA
IMAEV et al. (2003)
NERA
CHAI-YUREYA
145°
146°
147°
64°

Larina (1960) and Surmilova et al. (1986), Shilo (1961), Kurushin et al. (1976), and Imaev et al. (2003).

5.1.1 Larina (1960) and Surmilova et al. (1986) Variant

This configuration is a composite with the northern half derived from the geologic map of Surmilova et al. (1986), and the southern half derived from the older map of Larina (1960).

The relocated epicenters do not fit well to this mapping (Figure 5-1a). Epicenters northwest of Mt. Khulamrin are close to the Kobdi Fault, but not as close as in other versions of the Kobdi Fault. South of Mt. Khulamrin, the relocated epicenters take a sharp turn to the east, while the fault mapped in this variant steps to the west.

The Surmilova et al. (1986) mapping of the Kobdi Fault does not place it between Mt. Khulamrin and the detached diorite (Figures 2-2, 2-12), though the relocated epicenters clearly do.

The Larina (1960) and Surmilova et al. (1986) variant is the only one that suggests faults in the Upper Nera basin. Such faults could serve as a connection between the Kobdi and Arkagala faults. The faults shown in the variant (Figure 5-1a) are parallel and offset approximately 10 km to the southwest of the Kobdi Fault but appears to splay off of the Kobdi. Some of the earthquakes which plot in the Upper Nera basin fit close to this presumably buried fault.

5.1.2 Shilo (1961) Variant

The relocated epicenters fit very well to this mapping (Figure 5-1b). Epicenters that locate northwest of Mt. Khulamrin fall along or immediately adjacent to the Kobdi Fault. South of Mt. Khulamrin, the epicenters continue to follow the curved southern end of the Kobdi Fault, which has an approximate strike of 285-300°, and may meet up with the Mel'yankir Fault.

Fujita et al. (2002) suggested that the southern cluster was associated with the Mel'yankir Fault (section 2.2.6). Although some of the better located events do plot directly on the Mel'yankir fault, the totality of the data would seem to support their association with a curve to the east of the southern end of the Kobdi Fault. Regretably, the basis for why Shilo (1961) curved the south end of the Kobdi Fault is not stated, thus there is no way to evaluate the reasonableness of this mapping; surface features visible in satellite imagery are ambiguous (Figure 5-2).

The Shilo (1961) version of the Kobdi Fault and the epicenters aligning along it, clearly separates Mt. Khulamrin and the detached diorite.

The geometry of the faults as mapped by Shilo (1961) suggests that the Kobdi and Arkagala faults are distinct faults which are not connected to each other.

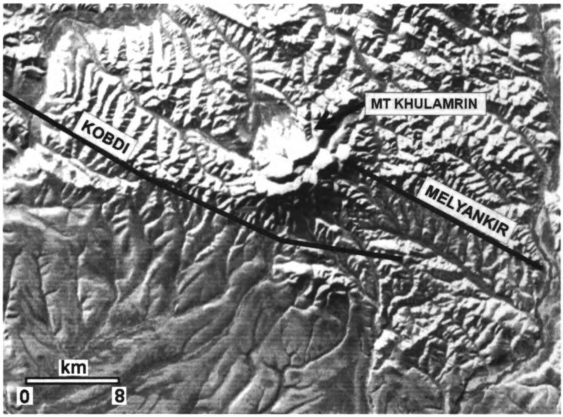

Figure 5-2. Satellite image of Mt. Khuramlin and vicinity showing the Shilo (1961) mapping of faults.

5.1.3 Kurushin et al. (1976) Variant

The relocated epicenters fit very well to this variant (Figure 5-1a), as the Kobdi Fault is very similar to that in Shilo (1961). Epicenters northwest of Mt. Khulamrin fall along or immediately adjacent to the Kobdi Fault, until reaching the Kobdi Stream area where most of the landslide activity occurred (section 2.1.5). The main difference between the Kurushin et al. (1976) and Shilo (1961) variants is that the Kobdi Fault continues with a strike of 315-320° within and northwest of the Kobdi Stream area in the Kurushin et al. (1976) map, whereas Shilo (1961) has the fault strike closer to 305-310°. There is only one mapped epicenter past this region, which fits the Shilo (1961) mapping, but there is not enough data to discriminate these variants. South of Mt. Khulamrin, the epicenters continue to follow the curved southern end of the Kobdi Fault, as in the Shilo (1961) map.

As with the Shilo (1961) map, the Kurushin et al. (1976) variant of the Kobdi Fault clearly separates Mt. Khulamrin and the detached diorite. Kurushin et al. (1976) maps the Arkagala Fault slightly different from Shilo (1961), however, it is clear that the two faults are distinct in both variants.

5.1.4 Imaev et al. (2003) Variant

Imaev et al. (2003) is the only variant that combines the Kobdi and Arkagala faults into a single Chai-Yureya Fault. The relocated epicenters fit their mapping of the Chai-Yureya Fault in the area immediately west and

northwest of Mt. Khulamrin, as it is identical to the Shilo (1961) and Kurushin et al. (1976) Kobdi Fault mappings. To the northwest, the Chai-Yuerya Fault of Imaev et al. (2003) is the same as Kurushin et al. (1976) and does not fit the data as well as Shilo (1961), although there are insufficient data to discriminate the two.

South of Mt. Khulamrin, the Imaev et al. (2003) map does not fit the aftershock data at all, as the epicenters take a sharp turn east, whereas their mapping of the Chai-Yureya Fault continues to the south-southeast. Imaev et al. (2003) map the Chai-Yureya Fault to the southwest of both Mt. Khulamrin and the detached diorite suggesting that the fault does not offset them. This is again discordant with the relocated epicenters.

The connection of the Kobdi and Arkagala faults as mapped by Imaev et al. (2003) is not only discordant with the aftershock distribution but with the apparent geology. This is further addressed in section 5.6.1.

Thus, the aftershock distribution is most consistent with the Kobdi fault as mapped by Shilo (1961) and suggests that there is no direct connection between the Kobdi and Arkagala faults in the Upper Nera basin.

5.2 Correlation of Aftershocks with Isoseismal Data

The intensity distribution of the Artyk main shock (see section 2.1.4) is oriented roughly southeast to northwest, with the long axis oriented 310-315°, coincident with the northwest cluster of the Artyk aftershocks in the vicinity of

Mt. Khulamrin. The region of maximum intensity as inferred from ground disruptions (Kobdi Stream valley; section 2.1.5) is located north of the region of maximal aftershock activity. Although Kochetkov and Koz'min (1976) suggested that the fact that the epicenter is located at one end of the aftershock zone and the maximum intensity is located at the other was significant (see section 2.1.5), this is most likely due to differences in ground conditions with widespread alluvial deposits in the Kobdi Stream valley which would be absent on the higher slopes of Mt. Khuramlin.

5.3 Temporal Distribution of Aftershocks

In section 4.4.2 it was noted that the station distribution varied considerably over time and that the highest quality events are concentrated in June and early July when the entire local network was operating. Because of this, assessing the temporal distribution of events over the entire aftershock sequence is skewed. Comparison of the epicentral distributions for May, June and July (Figure 4-8), shows that during the entire period, epicenters formed two groups to the northwest and southeast of Mt. Khuramlin, contrary to Kochetkov and Koz'min (1976), with variations in the amount of scatter about the Kobdi Fault. There does seem to be some decrease in the relative number of events in the southern cluster in July.

Detailed examination of subsets of the results from June and July show possible clusters, linear trends and variations in strike. However, it is impossible to tell if these are real based on the data available. The number of

events defining these clusters and trends is small (usually < 10) and could easily be due to differences in the reporting stations, as discussed in section 4.2.2, or unknown local variations in seismic velocities. Application of more sophisticated methods and careful, event by event, station by station analysis of the data are required to determine if these small-scale variations are real.

5.4 Outlier events

In the second half of June, there are three outliers (Figure 4-11) within 5 kilometers of the presumed trace of the Nera Fault (section 2.2.4) of Imaev et al. (2003) and Kurushin et al. (1976), near the channel of the Nera River and in the Upper Nera basin. These are high quality (groups 1 and 2) events, which suggests that their locations are relative accurate, they may have occurred on the Nera fault. There is only one teleseism that could be associated with this fault, which suggests that it is considerably less active at present that the Kobdi. Alternately, it is possible that these events are simply statistical outliers.

Additional outliers appear to form a trend between the Kobdi and Arkagala faults as mapped by Larina (1960) and Surmilova et al. (1986) in the southern Upper Nera basin (Figure 5-1a). Most of these events occurred in May (Figure 4-10), when the local network was not operating, which implies that the events locations may be less accurate. There are also no teleseisms which fall in this region within the Upper Nera basin, which indicates that such a fault within the basin, if it exists, is probably not as very active at present.

5.5 Magnitude versus Time

The number of aftershocks decreases with time (Figure 5-3; Kochetkov and Koz'min, 1976), but with an increase during the period the temporary network was operating reflecting a lower detection threshold.

The distribution of events by magnitude and location shows no biases; both clusters have roughly equal numbers of larger events (Figure 5-4).

5.6 Tectonic Implications of the Artyk Sequence

5.6.1 The Artyk Earthquake and Aftershocks

Based on the relocated mainshock epicenter and the aftershock sequence, the Artyk earthquake ruptured the southern part of the Kobdi Fault, with most of the rupture near Mt. Khulamrin. Although there is some scatter in the epicentral locations, within the estimated accuracy of the relocations (section 4.3) there is no compelling reason not to believe that the rupture is only on the Kobdi Fault; the aftershock sequence defines a relatively linear trend and does not show any obvious splays or secondary trends.

The depth resolution of the relocations is poor (the majority had to be fixed at 5 km as the calculated depth went above the surface or sub-crustal) but, taking the Russian determined depths (Figure 2-8) at face-value and combined with the focal mechanism (section 2.1.3), the Kobdi fault is a left-lateral strike-slip, nearly vertically dipping, fault. The bend in the

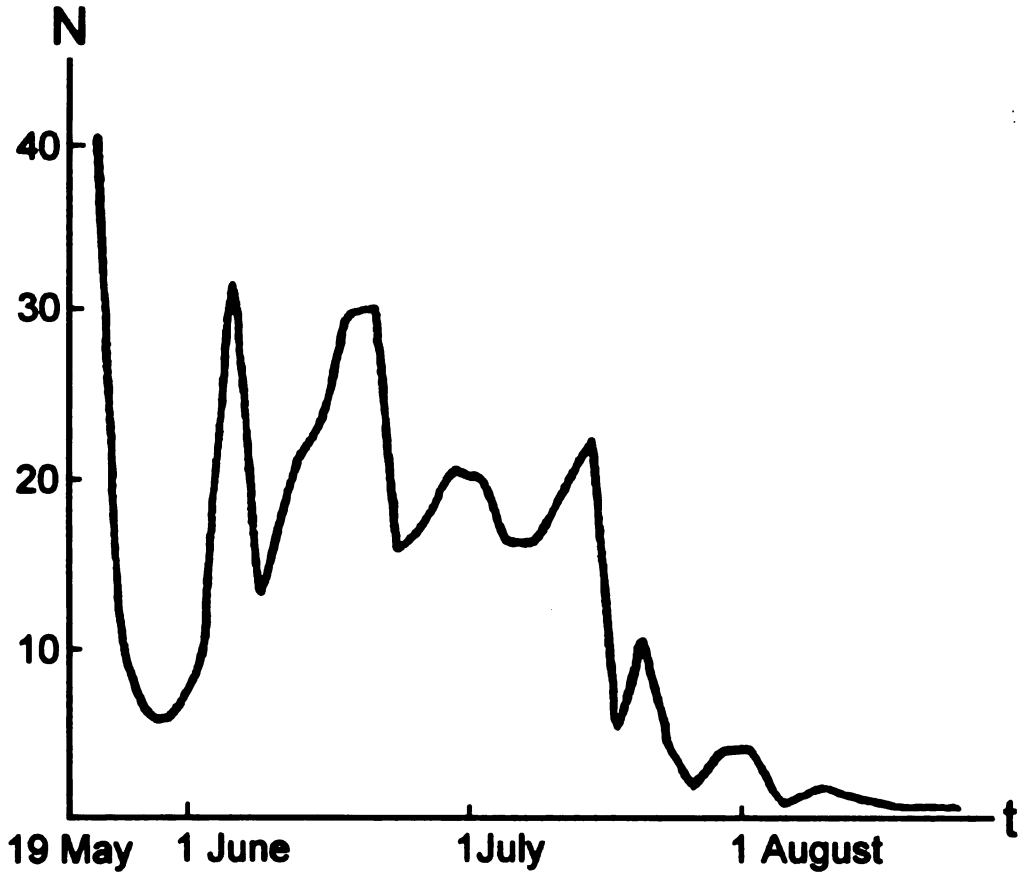

Figure 5-3. Distribution of aftershocks over time (after Kochetkov and Koz'min, 1976). The relative increase in June and early July reflects the time when the temporary stations were operational.

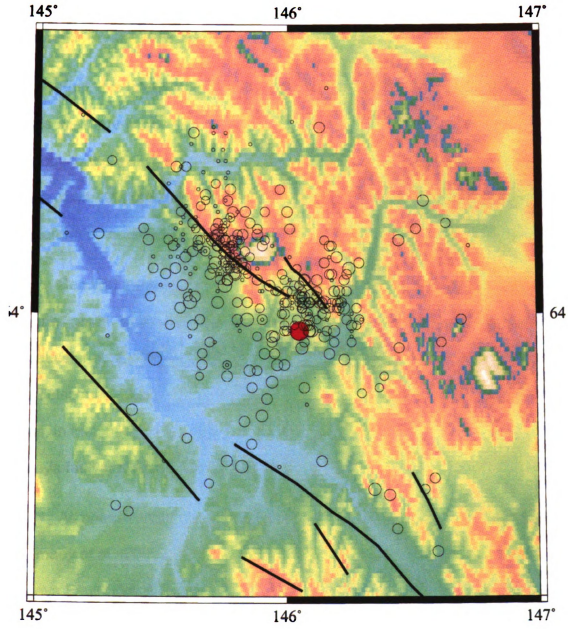

Figure 5-4. Relocated earthquakes plotted by magnitude. Red = main shock, M6.4. Aftershock earthquake magnitudes identified by diameter of circle.

aftershock sequence to the east south of Mt. Khulamrin into the valley of the Mel'yankir River can be interpreted in several ways.

First, it is possible that there is some systematic location bias for events in this area due to seismic velocity variations. This is unlikely in that the geology to the east and west of the Kobdi fault is the same to the north and south of Mt. Khulamrin (Surmilova et al., 1986), and the intrusion forming Mt. Khulamrin is too small to cause a significant location bias.

Second, the rupture may have splayed off onto a secondary fault in a manner similar to the later stages of the November 3, 2002, Denali earthquake (Haeussler et al., 2004), where the rupture diverted off the Denali and on to the Totschunda fault. This would allow a geometry in which the Kobdi Fault does, in fact, bend to the south to link with the Arkagala Fault (the Chai-Yureya fault system of Imaev et al., 2003).

As noted in section 2.2.3, however, this geometry which was suggested by Imaev et al. (2003), would result in a weak restraining bend in the Chai-Yureya Fault (Figure 2-13b). The region between the Kobdi Fault at Mt. Khulamrin and the Arkagala Fault south of Ozernoe form part of the Khudzhakh and Upper Nera basins (section 2.3.1) and is, in general, a topographic low area with no indications of recent compression or uplift visible in satellite imagery. If anything, the topography suggests a releasing bend.

Thus the Artyk earthquake and its aftershock sequence most likely ruptured only the Kobdi fault which bends to the southeast at its southern end.

5.6.2 Plate Tectonic Setting of the Artyk Earthquake Sequence

The lack of any visible faults or clear seismicity patterns in this area call into question whether the Kobdi and Arkagala faults join in this area. It further eliminates any possibility that a fault system exists that could curve to the southwest as required in the plate configuration model of Bird (2003) or the triple junction scenario of Imaev et al. (2003). All major faults either mapped by Russian geologists or interpreted from satellite imagery strike southeast (Figure 1-3; Imaev et al., 2000; Fujita et al., in press). This, plus the extremely odd geometry of the promontory of the Okhotsk plate (Figure 1-4b) argues strongly against the Artyk event having occurred on the Eurasia – Okhotsk boundary. In addition, if the Artyk earthquake were located on the Eurasia – Okhotsk plate boundary, the focal mechanism should be right-lateral along a roughly north-south plane; this is inconsistent with the well constrained solutions described in section 2.1.3.

The Kobdi Fault may curve slightly to the east into a zone of displacement that may act as a transfer between the Kobdi Fault and the Inyali-Debin Fault of Imaev et al. (1990, 1994, 2000) (Figure 1-3; Umar fault of Smirnov, 2000) some 50 km to the east. Some east-southeast striking lineations are visible in satellite imagery. The Inyali-Debin Fault is visible in satellite imagery and is also considered a left-lateral strike-slip fault (Imaev et al., 1990, 2000). Fujita et al. (2002) speculated that in such a scenario, the

Inyali-Debin fault, in association with other lineaments visible in satellite images could represent a fault system that could extend out into the Sea of Okhotsk and on to Kamchatka onto which the North America-Okhotsk plate boundary may be stepping. Field studies by Mackey et al. (2007, 2008b), however, conclusively demonstrate that the Ulakhan fault (section 2.2.2) is currently active in the Seimchan-Buyunda basin (Figure 1-3), thus there is no reason to postulate an alternative locus of displacement for the primary North America – Okhotsk boundary (Figure 1-4a).

Finally, since the Artyk event is offset over 100 km from the Ulakhan Fault, the event cannot be located on the present-day North America – Okhotsk boundary. The strike-slip nature of the mainshock and the linearity of the aftershock sequence, plus the lack of candidate faults that could link the Artyk epicentral region and the Ulakhan fault or the Ketanda fault system also precludes the suggestion of Imaev et al. (2003) that the Artyk sequence is located at the triple junction between the Okhotsk, North American and Eurasian plates (Figure 1-4c).

Previously, it was believed that the Okhotsk plate, while undergoing deformation was, on the whole, semi-rigid and undergoing extrusion by slip along highly conspicuous boundary faults such as the Ulakhan and the Ketanda (Figure 1-3). The location of the Artyk earthquake and the Chai-Yureya fault system, as mapped, however, are well-within the inside of the presumed Okhotsk plate as defined by most authors (e.g.,Parfenov et al.,

1988; Imaev et al., 2000; Fujita et al., 1997, in press). Given the location of the Artyk mainshock, if the Okhotsk plate was undergoing pure contraction, one would expect a fairly large earthquake, but with more of a thrust component. The pure strike-slip nature of the Kobdi Fault, however, suggests it is a major locus of deformation within the Okhotsk plate, likely due to nested extrusion or slivering of the northern Okhotsk plate in a manner modeled by Hindle et al. (2006, in press). This deformation could be taken up along several major strike-slip faults (Figure 1-4d), although the strike of the Kobdi/Chai-Yureya is different than sketched by Hindle (in press).

An examination of the general seismicity, teleseisms, and focal mechanisms of the continental part of the Okhotsk plate indicates that this model of accommodated deformation makes sense. The Artyk earthquake is a left-lateral strike-slip event which maps on the Kobdi fault, which may be a part of a greater Chai-Yureya fault system. Other left-lateral teleseismic events (e.g., June, 1985; June, 1970; January, 1972; December, 1986) have occurred on parallel and subparallel strike-slip faults within the Okhotsk plate (Figure 5-5). Many other left-lateral transpressional teleseismic events have occurred on the Ulakhan fault to the northeast, which clearly marks the NA-OK boundary, and to the southwest with right-lateral transpressional mechanisms on the Ketanda Fault, which marks the EU-OK boundary (Figure 1-3 and Figure 5-5; Riegel et al., 1993).

Figure 5-5. Seismicity and focal mechanisms of the northeast Russia study area. Major faults shown in black, earthquakes in green (scaled by magnitude). Focal mechanisms determined for earthquakes are shown in larger circles as lower hemisphere equal-area projections with compressional quadrants colored. Red events are well constrained, events in black are poorly constrained or of unknown quality. Dates are given for events with focal mechanisms and the Artyk earthquake is labeled.

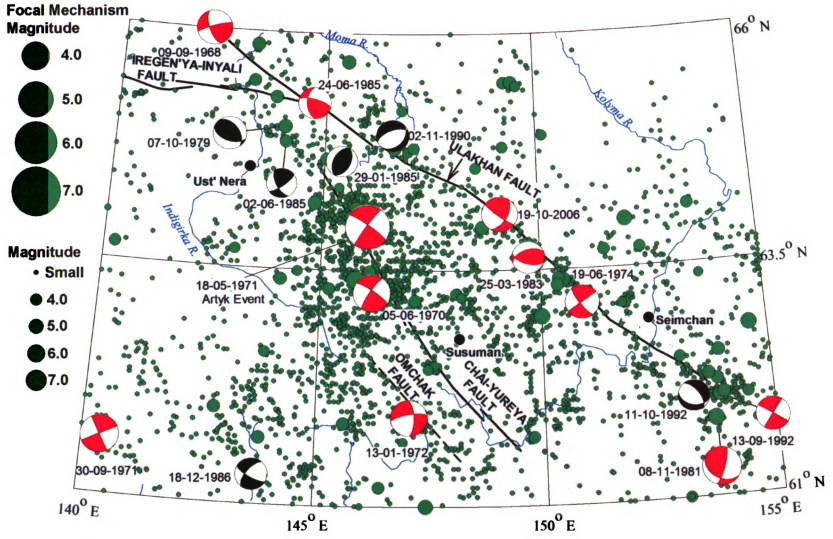
Focal Mechanism Magnitude
4.0
5.0
6.0
7.0
Magnitude
• Small
4.0
5.0
6.0
7.0
09-09-1968
IREGEN'YA-INYALI FAULT
24-06-1985
07-10-1979
Ust' Nera
02-06-1985
29-01-1985
02-11-1990
ULAKHAN FAULT
19-10-2006
Moma R.
Indigirka R.
Kolyma R.
18-05-1971
Artyk Event
05-06-1970
25-03-1983
19-06-1974
Seimchan
Susuman
OMCHAK FAULT
CHAL-YUREYA FAULT
11-10-1992
13-09-1992
08-11-1981
13-01-1972
30-09-1971
18-12-1986
66° N
63.5° N
61° N
140° E
145° E
150° E
155° E

The regional seismicity within the continental part of the Okhotsk plate (Figure 5-5), suggests that there are regions with elevated seismic activity, separated by relatively "quiet" zones which could indicate that there are some rigid slivers or blocks embedded within the deforming zone of the northern Okhotsk plate (Figure 1-2).

5.6.3 Displacement Rate on the Kobdi Fault

As discussed earlier, the aftershocks and the mapped trace (Shilo, 1961) of the Kobdi fault are located between the Mt. Khulamrin diorite and a detached diorite exposure south of it with an offset of 8 km in a left-lateral sense across the fault. If these represent parts of the same diorite and if the Kobdi fault also initiated movement at about the same time as the Ulakhan (c. 5 Ma; Fujita et al., in press), the slip rate is somewhat less than 0.2 cm/yr, or about one-third that of the Ulakhan.

5.6.4 Continuations of the Kobdi fault

5.6.4.1 Northwest Continuation

The relocated Artyk sequence clearly shows that the Chai-Yureya fault system ruptured in the vicinity of Mt. Khulamrin and along the Kobdi Fault to the northwest. Figure 2-10 shows that teleseismic seismicity occurs along an extrapolation of the Kobdi fault to the northwest, possibly trending well to the north of Ust' Nera. If this represents a continuation of the Kobdi fault then the Upper Nera basin is not now acting as a pull apart as suggested by Imaev et

al. (1990, 2000) and displacement is not transferred to the Nera Fault towards Ust' Nera (Figure 2-11).

5.6.4.2 Southeast Continuation

The seismicity, however, is not as clearly defined southeast of Mt. Khulamrin, and the Artyk aftershocks definitely do not occur on the Chai-Yureya fault as interpreted by Imaev et al. (2003).

The results of this study leaves open the question of whether the displacement is transferred back to the Arkagala fault through presently unknown faults, transferred to the Inyali-Debin to the east, or to some other fault. Also still unresolved is whether the fault, whether Arkagala or Inyali-Debin, is locked south of the Artyk epicentral zone and will rupture at a later date, or whether the strain is accommodated on a large number of small faults which will not generate a large earthquake. The recurrence interval on these faults is sufficiently long that it is likely we have not observed any significant portion of a full cycle of seismic activity.

Chapter 6: Conclusions

This study has analyzed a previously unavailable data set to relocate the aftershock sequence of a major earthquake in northeast Russia and to place the event in a plate tectonic context.

The Artyk earthquake occurred at 22 44 39.23 UTC on May 18, 1971, with an epicenter located at latitude 63.97°N and longitude 146.05°E, and a depth of 13 km. It had a moment magnitude, Mw, of 6.4 and released 10^{16} joules of energy. The epicenter was located to the south of Mt. Khulamrin, at the southern end of the aftershock sequence, supporting a propagation of the rupture to the north. The focal mechanism was left-lateral strike-slip along a fault plane striking 315° with a dip of nearly 90°.

The best-located aftershocks cluster very closely to the Kobdi fault as mapped by Shilo (1961), including a slight curve to the east to the south of Mt. Khulamrin. At this time, there is not enough information as to if and how the Kobdi Fault connects to the Arkagala fault and whether they form segments of a greater Chai-Yureya fault system, although the geometry of the southern part of the aftershock sequence suggests they may not be directly connected.

Almost all authors agree that the Ulakhan fault represents the primary locus of deformation between the North American and Eurasian plates over at least the past 5 million years (e.g., Imaev et al., 2000; Riegel et al., 1993; Fujita et al., in press). The location of the Artyk sequence clearly places it more than 100 km from the Ulakhan and onto a completely different fault. The field studies

of Mackey et al. (2007, 2008b) indicate the Ulakhan is presently active and mitigates against the proposal that the primary locus of displacement between North America and Okhotsk is shifting from the Ulakhan fault, thus the Artyk event is not associated with the North America – Okhotsk boundary (Figure 1-4a).

The Artyk earthquake is also not likely to have occurred on the Okhotsk – Eurasia plate boundary (Figure 1-4b). The earthquake clearly ruptures a fault with a strike near 300°, which would require the boundary to do a significant curve to realign with the known locus of displacement further south in the Ketanda fault zone (Parfenov et al., 1988; Riegel et al., 1993; Fujita et al., in press). Almost all significant mapped faults and lineaments continue the strike of the Kobdi (Chai-Yureya) fault in a southeast direction (Imaev et al., 1990, 2000; Fujita et al., in press) and no lineaments have been reported that strike southwest of the Artyk epicentral region. The focal mechanism is also inconsistent with this proposal.

The Artyk sequence ruptures along a known fault system in a linear, strike-slip manner and teleseisms align along it. There is no indication of a fault that would link the Kobdi (Chai-Yureya) to the Ulakhan and, as noted in the previous paragraph, it would be very difficult to link the Kobdi (Chai-Yureya) to the Ketanda system as well as having an inconsistent focal mechanism. Thus even if the locus of displacement were shifting from the Ulakhan to the Kobdi and

other fault systems, the Artyk sequence could not serve as a triple junction between the North American, Eurasian, and Okhotsk plates (Figure 1-4c).

Thus, of the possibilities presented in the introduction, the most likely is that the Kobdi (Chai-Yureya) represents an intraplate fault that is accommodating the convergence of North America and Eurasia by slivering and breaking up the northern part of the Okhotsk plate (Figure 1-4d) as suggested by Hindle et al. (in press). As the intraplate deformation is likely to be significantly slower than that on the boundaries, seismic activity would be infrequent and the presently known instrumental distribution represents a short snapshot of the activity; this is supported by the estimate of a displacement rate on the Kobdi of ~0.2 cm/yr. Other segments of this, or other faults, may rupture in the future. In any event, the northern part of the Okhotsk plate appears to be accommodating convergence by splintering into blocks separated by major strike-slip faults.

Further work with detailed field mapping, more refined relocation methods (e.g., double-difference; Waldhauser and Ellsworth, 2000), global positioning system surveys, will be necessary to resolve such questions as the nature and location of the continuation of the Kobdi Fault and its relationship to the Arkagala Fault. The 50 year instrumental period for seismology in northeast Russia represents only a fraction of the expected recurrence interval given the low slip rates, thus we have only recorded a snapshot of the deformation processes occurring in this complex region.

BIBLIOGRAPHY

Avetisov, G. P., 1993: Some aspects of lithospheric dynamics of Laptev Sea, *Izvestiya Physics of the Solid Earth*, 29, 402-412.

Avetisov, G. P., 1996: *Seismoactive Zones of the Arctic*, VNIIOkeanologiya, Sankt Peterburg. (in Russian)

Avetisov, G. P.: Yet again on the earthquakes of the Laptev Sea, *Geologo-Geofizichiskie Kharakhteristiki Litosfery Arkticheskogo Regiona*, 3, 104-113, 2000. (in Russian)

Bird, P., 2003: An updated digital model of plate boundaries, *Geochemistry Geophysics Geosystems*, v. 4(3), 1027, doi: 10.1029/ 2001GC000252

Balakina, L.M., Zakharova, A.I., Moskvina, A.G., and Chepkunas, L.S., 1993: Investigation of focal mechanisms of strong crustal earthquakes of northern Eurasia, 1927-1991, *Seismichhnost' i Seismicheskoe Raionirovanie Severnoi Evrazii*, 1, p. 123-131. (in Russian)

Bobrovnikov, V. A., and Izmailov, L. I., 1989: Present-day structure and geodynamics of the Earth's crust of the southeastern part of the Yana-Kolyma system, in Lin'kova, T. I., and Krasnyi, L. L., eds, *Geophysical Investigations for the Solution of Geologic Problems*, SVKNII DVO AN SSSR, Magadan, 5-23. (in Russian).

Calais, E., DeMets, C., and Nocquet, J.-M., 2003: Evidence for a post-3.16-Ma change in Nubia-Eurasia-North America plate motions? *Earth and Planetary Science Letters*, 216, 81-92.

Chapman, M.E., and Solomon, S.C., 1976: North American – Eurasian plate boundary in northeast Asia, *Journal of Geophysical Research*, 81, 921-930.

Cherepovsky, V. F., ed., 1999: *Coal Basins and Deposits of the Far East, Coal basis of Russia*, v. 5, book 2, ZAO Geoinformmark, Moscow. (in Russian)

Cochran, J. R., Kurras, G. J., Edwards, M. H., and Coakley, B. J., 2003: The Gakkel Ridge: Bathymetry, gravity anomalies, and crustal accretion at extremely slow spreading rates, *Journal of Geophysical Research*, 108, doi:10.1029/2002JB001830, 2003.

Cook, D. B., Fujita, K., and McMullen, C. A., 1986: Present-day plate interactions in northeast Asia: North American, Eurasian, and Okhotsk plates, *Journal of Geodynamics*, 6, 33-51.

Davydova, N. I., Shvarts, Y. B., and Yaroshevskaya, G. A., 1968. Wave patterns in deep seismic sounding along the Magadan-Kolyma profile, in Deep Seismic Soundings of the Earth's Crust in the USSR: *International Geology Review* – Book Section, 10, 93-102.

Douglas, A., 1967: Joint epicenter determination, *Nature*, 215, 47-48.

Engdahl, E. R., van der Hilst, R. D., and Buland, R., 1998: Global teleseismic earthquake relocation with improved travel times and procedures: *Bulletin of the Seismological Society of America*, 88, 722-743.

Engen, Ø., and Eldholm, O., 2003: The Arctic plate boundary, *Journal of Geophysical Research*, 108(B2), 2075, doi:10.1029/2002JB001809, 17 pp.

England, P., and Jackson, J., 1989: Active deformation in the continents, *Annual Reviews of Earth and Planetary Science*, 17, 197-226.

Filson, J., and Frasier, C. W., 1972: The source of a Siberian earthquake, *Eos Transactions of the American Geophysical Union*, 53, 1041.

Franke, D., Krüger, F., and Klinge, K., 2000: Tectonics of the Laptev Sea - Moma 'Rift' region: investigation with seismologic broadband data, *Journal of Seismology*, 4, 99-116, 2000.

Fujita, K., Cook, D. B., Hasegawa, H., Forsyth, D., and Wetmiller, R., 1990a: Seismicity and focal mechanisms of the Arctic region and the North American plate boundary in Asia, in Grantz, A., Johnson, G. L., and Sweeney, J. F., eds., *The Geology of North America, v. L., The Arctic Region*, Geological Society of America, Boulder, 79-100.

Fujita, K., Cambray, F. W., and Velbel, M. A., 1990b: Tectonics of the Laptev Sea and Moma rift systems, northeastern USSR, *Marine Geology*, 93, 95-118.

Fujita, K., Stone, D. B., Layer, P. W., Parfenov, L. M., and Koz'min, B. M., 1997: Cooperative program helps decipher tectonics of northeast Russia, *Eos Transactions of the American Geophysical Union*, 78, 245, 252-253.

Fujita, K., McLean, M. S., Mackey, K. G., and Kozmin, B. M., 2002b: The 1971 Artyk earthquake: Is the locus of motion changing in northeast Russia? *Eos Transactions of the American Geophysical Union*, 83(47), suppl., F1247.

Fujita, K., Sella, G., Mackey, K. G., Stein, S., Park, K.-D., and Imaev, V. S., 2004: Relationships between seismicity and GPS determined velocities in northeast Asia, *Eos Transactions of the American Geophysical Union*, 85(47), suppl., F667.

Fujita, K., Koz'min, B. M., Mackey, K. G., Riegel, S. A., McLean, M. S., and Imaev, V. S., in press: Seismotectonics of the Chersky Seismic Belt, eastern Sakha Republic (Yakutia) and Magadan District, Russia, in Stone, D. B., editor in Chief, *Northeastern Russia, Geology, Geophysics and Tectonics: A tribute to Leonid Parfenov*, Stefan Mueller series, EGS.

Gorodinsky, M. E., ed., 1982: *Geologic Map of the Northeast USSR*. Vsesoyuz Nauchnyi-Issledovatel'sky Geologichesky Institut, Leningrad, scale 1:5,000,000 (dated 1980). (in Russian)

Gordon, R. G., 1998: The plate tectonic approximation: Plate nonrigidity, diffuse plate boundaries, and global plate reconstructions, *Annual Reviews of Earth and Planetary Science*, 26, 615-642.

Grinenko, O. V., Sergeenko, A. I., and Belolyubsky, I. N., 1998b: *Paleogene and Neogene of Northeastern Russia*, Part II, Izd-vo YNTs SO RAN, Yakutsk, 57 pp. + 36 p. supplement volume. (in Russian)

Gusev, G. S., 1979: *Folded Structures and Faults of the Verkhoyansk-Kolyma System of Mesozoides*, Nauka, Moscow, 206 pp. (in Russian)

Gusev, G. S., Mokshantsev, K. B., and Tret'yakov, F. F., 1976: Faults of the Verkhoyansk-Chukotka folded region, in Mokshantsev, K. B., ed., *Fault Tectonics of the Territory of the Yakut ASSR*, Izdanie Yakutskogo Filiala SO AN SSR, Yakutsk, 73-114. (in Russian)

Haeussler, P. J., Schwartz, D. P., Dawson, T. E., Steuner, H. P., Lienkaemper, J. J., Sherrod, B., Cinti, F. R., Montone, P., Craw, P. A., Crone, A. J., and Personius, S. F., 2004. Surface rupture and slip distribution of the Denali and Totschunda faults in the 3 November 2002 M 7.7 earthquake, Alaska, *Bulletin of the Seismological Society of America*, v. 94(6B) p. S23-S52.

Hindle, D., Fujita, K., and Mackey, K.: Current deformation rates and extrusion of the northwestern Okhotsk plate, northeast Russia, *Geophysical Research Letters*, 33, doi:10.1029/2005GL024814, 2006.

Hindle, D., Fujita, K., and Mackey, K., in press: Deformation of the northwestern Okhotsk plate. How is it happening? in Stone, D. B., editor in chief, *Northeastern Russia, Geology, Geophysics and Tectonics: A tribute to Leonid Parfenov*, Stefan Mueller series, EGS.

Imaev, V. S., Imaeva, L. P., and Koz'min, B. M., 1990: *Active Faults and Seismotectonics of Northeast Yakutia*, Yakutskii Nauchnyi Tsentr SO AN SSSR, Yakutsk. (in Russian)

Imaev, V. S., Imaeva, L. P., Koz'min, B. M., and Fujita, K., 1994: Active faults and recent geodynamics of Yakutian seismic belts, *Geotectonics*, 28, 146-158.

Imaev, V. S., Imaeva, L. P., and Koz'min, B. M., 2000: *Seismotectonics of Yakutia*, GEOS, Moscow. (in Russian)

Imaev, V. S., Imaeva, L. P., and Koz'min, B. M., 2003: Dynamics of seismotectonic processes in the zone of articulation between the Eurasian, North American, and Okhotsk Sea plates (northeast Asia), *Otechestvennaya Geologiya*, 2003(6), p. 69-74. (in Russian)

Jackson, J., and McKenzie, D., 1988: The relationship between plate motions and seismic moment tensors, and the rates of active deformation in the Mediterranean and Middle East, *Geophysical Journal*, 93, 45-74.

Jeffreys, H., and Bullen, K. E., 1940. *Seismological Tables*, British Association for the Advancement of Science, London, 50 pp.

Kennett, B. L. N., 1991. *IASPEI 1991 Seismological Tables*: Research School of Earth Sciences, Australian National University, Canberra, 167 pp.

Kochetkov, V. M., and Koz'min, B. M., 1976: The Oimyakon earthquake of 1971 and its aftershocks, in Solov'ev, S. L., editor in chief, *Seismicity and Deep Structure of Siberia and the Far East*, DVNTs AN SSSR, Vladivostok, p. 61-67. (in Russian)

Kondorskaya, N. V., and Shebalin, N. V., eds., 1977: *New Catalog of Strong Earthquakes in the Territory of the USSR From Ancient Times to 1977*: Nauka, Moscow, 534 pp.

Korol'kov, V. G., 1992: *State Geologic Map, sheet O-56 (Magadan), P-56, 57 (Seimchan)*, VSEGEI, Sankt-Peterburg, scale 1:1,000,000. (in Russian)

Koz'min, B. M., 1984: *Seismic Belts of Yakutia and the Focal Mechanisms of Their Earthquakes*, Nauka, Moscow. (in Russian)

Koz'min, B. M., Emel'yanov, N. P., Emel'yanova, A. A., Zhelinskaya, E. A., Larionov, A. G., and Kim, V. F., 1975: Strong earthquakes of Yakutia, in Gorbunova, I. V., Kondorskaya, N. V., and Shebalin, N. V., eds., *Earthquakes of the USSR in 1971*, Nauka, Moscow, p. 133-141. (in Russian)

Kroeger, G. C., 1987: *Synthesis and Analysis of Teleseismic Body Wave Seismograms*, Ph.D. Dissertation, Stanford University, Stanford.

Kurushin, R. A., Dem'yanovich, M. G., and Kochetkov, V. M., 1976: Macroseismic manisfestations of the Oimyakon earthquake, in Solov'ev, S. L., editor in chief, *Seismicity and Deep Structure of Siberia and the Far East*, DVNTs AN SSSR, Vladivostok, p. 50-60. (in Russian)

Larina, N. I., 1960. *State Geologic Map of the USSR, sheet P-55 (Kolyma River)*, Ministerstvo Geologii i Okhrany Nedr SSSR, (Leningrad), scale 1:1,000,000. (in Russian)

Mackey, K. G., 1999: *Seismological Studies in Northeast Russia*, Ph.D. Dissertation, Michigan State University, East Lansing.

Mackey, K. G., and Fujita, K., 1999: The northeast Russia seismicity database and explosion contamination of the Russian earthquake catalog, in *Proceedings of the 21st Seismic Research Symposium: Technologies for monitoring the Comprehensive Nuclear-Test-Ban Treaty*, v. 1, US Department of Defense, LA-UR-99-4700, 151-161.

Mackey, K., and Fujita, K., 2001: Seismic calibration and discrimination in northeast Russia, in *Proceedings of the 23rd Seismic Research Review: Worldwide Monitoring of Nuclear Explosions*, v. 1, National Nuclear Safety Administration, US Department of Energy, 80-89.

Mackey, K. G., Fujita, K., Gunbina, L. V., Kovalev, V. N., Imaev, V. S., Koz'min, B. M., and Imaeva, L. P., 1997: Seismicity of the Bering Strait region: Evidence for a Bering Sea block, *Geology*, 25, 979-982.

Mackey, K. G., Fujita, K., Gounbina, L., Koz'min, B., Imaev, V., Imaeva, L., and Sedov, B., 2003: Explosion contamination of the northeast Siberian seismicity catalog: implications for natural earthquake distributions and the location of the Tanlu fault in Russia, *Bulletin of the Seismological Society of America*, 93, 737-746.

Mackey, K. G., Hampton, B. A., Fujita, K., Kurtkin, S., and Gounbina, L. V., 2007: Active faulting along the Ulakhan Fault, Seimchan-Buyunda basin, northeast Russia, *Eos Transactions of the American Geophysical Union*, 88(52), suppl., T13D-1579.

Mackey, K., Fujita, K., Hartse, H. E., Steck, L. K., Gounbina, L., Leyshuk, N., Shibaev, S., Koz'min, B., Imaev, V., Gordeev, E., Masalski, O., Gileva, N., Bormotov, V.A., and Voitenok, A.A., 2008a: *Seismicity of Eastern Russia 1960-2007*, LAUR-04-1381, 1 sheet.

Mackey, K. G., Hampton, B., Fujita, K., Koz'min, B. M., Shibaev, S. V., and Gounbina, L. V., 2008b: Field studies of active fault zones in eastern Russia, in Malovichko, A. A., ed., *Seismicity of Northern Eurasia*: Geophysical Survey RAS, Obninsk, p. 200-204.

Mal'kov, B. I., 1969: Structure and development of the Lyglykhtakh late geosynclinal depression, in *Mesozoic Tectonogenesis (Proceedings of the VII Session Scientific Council on the Tectonics of Siberia and the Far East)*, SVKNII, Magadan, p. 74. (in Russian)

Mal'kov, B. I., 1971: Scheme of development of the southeastern part of the Yana-Kolyma geosynclinal system, in *Mesozoic Tectonogenesis*, SVKNII DVO AN SSSR, Magadan, 43-50. (in Russian)

McLean., M. S., Fujita, K., Mackey, K. G., Kleber, E., Koz'min, B. M., and Imaev, V.S., 2000: The Ulakhan fault system, northeast Russia, *Eos Transactions of the American Geophysical Union*, 81(48), suppl., F1164.

McMullen, C. A., 1985: *Seismicity and Tectonics of the Northeastern Sea of Okhotsk*, M.S. Thesis, Michigan State University, East Lansing.

Newman, A. V., and Okal, E. A., 1998: Teleseismic estimates of radiated seismic energy: The E/Mo discriminant for tsunami earthquakes, *Journal of Geophysical Research*, v. 103, p. 20885-20898.

Nokleberg, W. J., Parfenov, L. M., Monger, J. W. H., Norton, I. O., Khanchuk, A. I., Stone, D. B., Scotese, C. R., Scholl, D. W., and Fujita, K., 2000: Phanerozoic tectonic evolution of the circum-north Pacific, *U. S. Geological Survey Profesional Paper* 1626.

Okal, E. A., and Talandier, J., 1989: Mm: A variable-period mantle magnitude, *Journal of Geophysical Research*, 94, 4169-4193.

Parfenov, L. M., 1991: Tectonics of the Verkhoyansk-Kolyma Mesozoides in the context of plate tectonics, *Tectonophysics*, 199, 319-342.

Parfenov, L. M, and Kuz'min, M. I., eds., 2001: *Tectonics, Geodynamics, and Metallognesis of the Territory of the Sakha Republic (Yakutia)*, MAIK Nauka/Interperiodika, Moscow, 570 pp. (in Russian)

Parfenov, L. M., Koz'min, B. M., Grinenko, O. V., Imaev, V. S., and Imaeva, L. P., 1988: Geodynamics of the Chersky seismic belt, *Journal of Geodynamics*, 9, 15-37.

Pedoja, K., Bourgeois, J., Pinegina, T., and Higman, B., 2006: Does Kamchatka belong to North America? An extruding Okhotsk block suggested by coastal neotectonics of the Ozernoi Peninsula, Kamchatka, Russia, *Geology*, 34, 353-356.

Pujol, J., 2000. Joint event location – the JHD technique and applications to data from local seismic networks, in Thurber, C. H., and Rabinowicz, N., eds., *Advances in Seismic-Event Location*, Kluwer Academic, Dordrecht, 163-204.

Rautian, T. G., Khalturin, V. I., Fujita, K., Mackey, K. G., and Kendall, A. G., 2007: Origins and methodology of the Russian energy K-class system and its relationship to magnitude scales, *Seismological Research Letters*, 78, 579-590.

Riegel, S. A., 1994: *Seismotectonics of Northeast Russia and the Okhotsk Plate*, M.S. Thesis, Michigan State University, East Lansing.

Riegel, S. A., Fujita, K., Koz'min, B. M., Imaev, V. S., and Cook, D. B., 1993: Extrusion tectonics of the Okhotsk plate, northeast Asia, *Geophysical Research Letters*, 20, 607-610.

Savostin, L. A., and Karasik, A. M., 1981: Recent plate tectonics of the Arctic basin and of northeastern Asia, *Tectonophysics*, 74, 111-145.

Savostin, L. A., Verzhbitskaya, A. I., and Baranov, B. V.: Present-day tectonics of the Sea of Okhotsk plate region, *Doklady Akademii Nauk SSSR*, 266, 961-965, 1982. (in Russian)

Savostin, L., Zonenshain, L., and Baranov, B.: Geology and plate tectonics of the Sea of Okhotsk, *American Geophysical Union Geodynamics Series*, 11, 189-221, 1983.

Schlindwein, V., Müller, C., and Jokat, W., 2007: Microseismicity of the ultraslow-spreading Gakkel ridge, Arctic Ocean: a pilot study, *Geophysical Journal International*, 169, 100-112.

Sella, G. F., Dixon, T. H., and Mao, A., 2002: REVEL: A model for Recent plate velocities from space geodesy, *Journal of Geophysical Research*, 107, doi:10.1029/2000JB000033.

Shilo, N. A., 1961. Quaternary deposits of the Yana-Kolyma auriferous belt, conditions and stages of its formation, *Trudy VNII-1*, 66, 136 pp. (in Russian)

Smirnov, V. N., 2000: Orogenic Regions, northeast Eurasia, in Grachev, A. F., ed., *Neotectonics, Geodynamics, and Seismicity of Northern Eurasia*, PROBEL, Moscow, 120-133. (in Russian)

Smirnov, V.N. and Levashova, S.V., 1988: Strong earthquakes of the northeast USSR according to interpretation of space and air photos, in Sidorov, A.A., Izmailov, L.I., Lin'kova, T.I. and Silant'er, V.N., eds., *Nature of Geophysical Fields of the Northeast USSR*: SVKNII DVO AN SSSR, Magadan, p39-53. (in Russian)

Spence, W., 1980: Relative epicenter determination usiong P-wave arrival-time differences, *Bulletin of the Seismological Society of America*, 70, 171-183.

Steblov, G. M., Kogan, M. G., King, R. W., Scholz, C. H., Bürgmann, R., and Frolov, D. I., 2003: Imprint of the North American plate in Siberia revealed by GPS, *Geophysical Research Letters*, 30, doi:10.1029/2003GL017805.

Steck, L. K., Phillips, W. S., Mackey, K., Begnaud, M. L., Stead, R. J., and Rowe, C. A., 2009. Seismic tomography of crustal P and S across Eurasia: *Geophysical Journal International*, 177, 81-92.

Surmilova, E. P., Maksimova, G. A., and Natapov, L. M., 1986. *State Geologic Map of the USSR, sheet Q-54,55 (Khonuu)*, VSEGEI, Leningrad, scale 1:1,000,000 (dated 1985). (in Russian)

Tret'yakov, F.F., 2003. Darpir and Ulakhan Faults: Contemporary Interpretation: *Otechestrennaya Geologiya*, 2003 (6), p. 78-80. (in Russian)

Vashchilov, Y. Y., 1963: Deep faults of the southern Yana-Kolyma fold zone and the Okhotsk-Chaun volcanic belt and their role in the formation of granitic intrusions and the formation of structures (according to geophysical data), *Sovetskaya Geologiya*, 1963(4), p. 54-72. (in Russian)

Vogt, P. R., Taylor, P. T., Kovacs, L. C., and Johnson, G. L., 1979: Detailed aeromagnetic investigation of the Arctic basin, *Journal of Geophysical Research*, 84, 1071-1089.

Yang, X., Bondár, I., and Romney, C., 2000: *PIDC Ground Truth Event (GT) Database (Revision 1)*: CMR Technical Report CMR-00/15, 14 pp.

Waldhauser and Ellsworth, 2000: A Double-Difference Earthquake Location Algorithm: Method and Application to the Northern Hayward Fault, California, *Bulletin of the Seismological Society of America*, 90, 1353-1368.

Wells, D. L., and Coppersmith, K. J., 1994: New empirical relationships among magnitude, rupture length, rupture width, rupture area, and surface displacement, *Bulletin of the Seismological Society of America*, 84, 974-1002.

Wilson, J. T., 1963: Hypothesis of Earth's behaviour, *Nature*, 198, 925-929.